Cultivation of Natural Killer Cell for Immunotherapy

A THESIS
SUBMITTED TO THE FACULTY OF THE
UNIVERSITY OF MINNESOTA
BY

Hansol Kim

IN PARTIAL FULFILLMENT OF THE REQUIREMENTS
FOR THE DEGREE OF
MASTER OF SCIENCE

Advisor: Professor Wei-Shou Hu

April 2018

ACKNOWLEDGEMENT

I would like to take this opportunity to thank all people who helped me throughout the Master's studies at the University of Minnesota.

Before I came to Minnesota, my interest for the future did not reach beyond biologics manufacturing. However, Professor Wei-Shou Hu changed the way I envision my career as well as the industry. He will be the first one to thank for my future career in biopharmaceutical industry. Without his foresight and toughness, I would not be able to even learn about cellular immunotherapy that has so much potential in the future. I would like to thank for his toughness and demand for perfection as well as occasional encouraging words.

I would also like to thank Professor Frank Cichocki to collaborate with his research group. While I stayed in his laboratory for the most of my studies, all achievements would not be able to become reality without help from fellow researchers, Bin Zhang, Hongbo Wang, Cheng-Ying Wu, Emily Taras, Phillip Dougherty, and Katie Tuininga.

It was not an easy task to combine knowledge from the field of immunology and chemical engineering. Every time I was having hard time interpreting the two different sciences, every single individual from Wei-Shou Hu research group gave me lots of help. I would like to thank Chris Stach, David Chau, Arpan Bandyopadhyay, Tung Le, Sofie O'Brien, Conor O'Brien, Meghan McCann, Kevin Ortiz-Rivera, Jen One, Zion Lee, and Thu Phan. I would also like to thank Victoria Roberts for her expertise in graphics design.

Lastly, nearly two years of journey could not be finished without my beloved wife, Saem Heo, and my son, Daon Kim. It looked almost impossible doing graduate studies together with my wife, but we eventually made it.

My family had received tremendous amount of support from the state of Minnesota. All forms of support, both financially and institutionally, were heartily appreciated.

DEDICATION

To my beloved wife, Saem, and son, Daon.

ABSTRACT

Natural Killer (NK) cells are a type of blood immune cells that are capable of lyse the infected or transformed cells without prior sensitization. Due to a small fraction of NK cells within human bodies, and the fact that the cells are not able to expand to lyse the target cells, cells were isolated from human blood, and were expanded. NK cells expanded without feeder cells showed only a small number of fold expansion. However, when the NK cells were co-cultivated with artificial Antigen Presenting Cells (aAPCs), NK cells showed a much greater number of fold expansion. Especially, NK cells co-cultured with K562 cells with membrane bound IL-21 (K562.mbIL21) showed about 10,000-fold expansion for 14 days cultivation. Continuous cultivation of NK cells with the K562.mbIL21 showed more than 100 billion-fold expansion for 30 days before it shows senescence. By employing a multivariate analysis technique, phenotypic changes during the activation and expansion of NK cells were captured. In addition, various kinetic parameters during the cultivation were identified to provide preliminary data for future research. It was found that NK cells could expand with dead aAPCs and their debris, showing a possibility of expanding NK cells without feeder cells since the K562 cells are cancerous, thus, they need to be completely removed for clinical use in promoting NK cells in the field of adoptive immunotherapy.

TABLE OF CONTENTS

LIST OF TABLES

LIST OF FIGURES

1 INTRODUCTION

1.1 CELL THERAPY

Cell therapy is a method of treating diseases using living whole cells by administering the cells to patients suffering from many genetic disorders and some acquired ones. It aims to target various cellular diseases by certain cell populations or carrying cells that can be used for therapeutic use. In addition to cell therapy, gene therapy has brought tremendous influence in the development of genetic modifications on cells for treatment purposes. Two fields of gene and cell therapy have created such a synergy for unmet medical needs.

Cells used for the cell therapy can be originated from either a patient (autologous) or a donor (allogeneic). Blood infusions are considered the first generation of cell therapy and are now everyday practices. Bone marrow transplantation is another type of cell therapy started in early days to treat disease like cancer and immunodeficiency. Nowadays, cell therapy is expanding to utilize more types of cells including stem cell, T cell and Natural Killer cell.

1.2 APPLICATION OF CELL THERAPY (CAR-T AND NK)

Among a few recent advancements in medicine, cancer immunotherapy has achieved the most advances in terms of the amount of research that has been done, and the number of ongoing clinical trials (J. F. Miller & Sadelain, 2015). T-cell immunotherapy has shown tremendous success treating certain types of cancers, such as lymphoma, leukemia, and melanoma. Autologous T cells are obtained from patient's blood, and are engineered so that the T cells will be

redirected to specifically target cancer cells in the patient's body. Then, the engineered T cells are infused back to the patient (Couzin, 2002). By doing the engineering of the T cells using gene editing techniques, it will enhance the capability to kill the target cell more efficiently. One of the technique involves expressing receptors like chimeric antigen receptors (CARs). The CARs are composed of an antigen recognition domain from monoclonal antibody and a domain that is responsible for T cell signaling and co-stimulation. Those CAR T cells have shown efficacy to treat B-cell malignancy by targeting the CD19 cell surface antigen (Levine, Miskin, Wonnacott, & Keir, 2017). The first CAR-T cell therapy was approved in 2017 by Novartis. More and more CAR-T therapies targeting different types of cancers are under clinical trials.

Natural Killer (NK) cells play important roles in human by initiating responses to infections, such as influenza, cytomegalovirus (CMV), herpes simplex virus (HSV), and respiratory syncytial virus. The potential of NK cell due to its antiviral, anti-graft-versus-host disease, and anti-cancer functionality, it is expected that NK cells can be used to treat certain indications, including sarcomas, myeloma, carcinomas, lymphomas, and leukemias (Denman et al., 2012).

There are a few challenges that NK cell therapy have to overcome. It is important to understand NK cell biology fully so that NK cells can be manufactured with highest cytotoxicity possible for use in clinical applications (Koepsell, Miller, & McKenna, 2013). Once the variables that contribute to the NK cell activation, the cells need to be expanded with persistence for commercial manufacturing.

1.3 NEED OF SCALABILITY AND SCALE UP

Most CAR-T therapies that are either approved or in clinical trial employ autologous T cells, meaning T cells from the patient himself/herself. Because of high efficacy of CAR-T cells derived from autologous T cells, there is no need for a large number of T cells during the cell engineering. Despite of the fact that autologous CAR-T therapy has shown superior results compared to allogeneic CAR-T therapy, there are allogeneic CAR-T therapies under clinical trials. One limitation for the allogeneic therapy is coming from difficulty to expand the number of cells *ex vivo* (Vera et al., 2010; Yang, Jacoby, & Fry, 2015). While autologous therapy is for only one patient, allogenic therapies need to provide sufficient number of cells for multiple patients.

Such needs for rapid expansion are also of utmost concern for NK cell therapy. Compared to T cells that dominate within the lymphocytes, NK cells comprise of only 5-15% of human lymphocytes that limited number of NK cells can be obtained from a single donor or patient. In case of a single clinical trial for 100 patients, each patient needs at least a single infusion of 2×10^7 NK cells/kg (Meyer-Monard et al., 2009). Assume each patient weighs 100 kg, NK cells need to be expanded to 2×10^{11} NK cells to provide a sufficient number of cells for a single trial. In case multiple infusions are needed throughout the treatment, the total number of NK cell needs to be multiplied by the number of infusion.

Moreover, *ex vivo* scale up of NK cell expansion is not only needed for a large number of cells for therapy, but also for priming NK cells that were resistant to lyse the target cells. Generally, NK cells are not showing good functionality within

human body, prior to priming, because their activating receptors are downregulated. *Ex vivo* expansion with certain combination of cytokines will greatly enhance the cytotoxicity against tumors. It is now clear that there needs a method to expand NK cells sufficiently to meet the needs in both clinical and commercial scale, and also enhance the function against immunosuppression (Granzin et al., 2017).

2 BACKGROUND

2.1 BACKGROUND: WHAT IS A NK CELL?

Natural Killer (NK) cells belong to a distinct subset of large granular lymphocytes within the human immune system. Because of its innate nature rather than adoptive, the name itself had been derived from its cytolytic function that mediates spontaneous and nonspecific lysis of target cells without any priming. One major difference between T cell and NK cell is how NK cells recognize the target cell. Thanks to Major Histocompatibility Complex (MHC) molecules expressed on the surface of cells that are either transformed or virus infected, NK cells can recognize the cells that lacks the MHC molecules for lysis (Ljunggren & Karre, 1990).

There are about two billion NK cells flowing around in a human body. From a traditional point of view, NK cell can be defined as a cell phenotype expressing CD56, a 140-kDa isoform of cell adhesion molecule (NCAM) found on NK cells, and lacks CD3, a T cell marker. Therefore, by using flow cytometry, a gate can be applied to include NK cells while excluding T cells. While CD56+CD3- phenotype still defines a NK cell nowadays, Vivier has suggested using NKp46, a natural cytotoxicity receptor (NCR) family that belongs to activating receptor, as a defining phenotype of NK cell (Walzer, Jaeger, Chaix, & Vivier, 2007)

NK cells secrete cytokines and chemokines that affect the host's immune response and have a capability to lyse certain infected and transformed cells by perforin and granzyme. NK cells also induce the death of target cells by inducing death receptor related pathways, such as Fas and TRAIL (Smyth et al., 2005). There are two distinguished subsets of NK cells. $CD56^{bright}$CD16- population shows mostly

immune modulatory function by secreting interferon (IFN)-g. CD56dimCD16+ population shows direct cytotoxic functionality by secreting perforin and granzyme (Vivier, Tomasello, Baratin, Walzer, & Ugolini, 2008).

2.2 CELL THERAPY PROCESS (CULTIVATION, FREEZE, THAW)

There are different culture systems that can culture NK cells *ex vivo*. The size of the system typically depends on the purpose of the system as well as the number of cells needed.

In research laboratories where testing various conditions is the purpose of the culture, cell culture plates and T flasks are used for pre-clinical experiments. However, due to the small volume of each condition, cell culture plates and T flasks are difficult to produce enough number of cells for clinical purposes. For expansion purposes, it takes as much as 51 T flasks to produce NK cells that can be used for just a single dose (Parkhurst, Riley, Dudley, & Rosenberg, 2011). As the number of flasks increases, more manual manipulations are needed to culture cells for exchanging media and harvesting the cells for passaging. It will eventually increase a risk of contamination during the process that it is not an idealistic method for NK cell expansion for clinical purposes.

Disposable bags can be used for NK cell expansion. Because the volume of a bag can be much larger than its T flask counterpart, much larger number of cells can be obtained. While cells settle down at the bottom of the bag, media in the bag can be changed using a tubing at the top of the bag making the overall process easier.

By using disposable bags, all tubings can be welded without breaking the sterile boundary so that the risk of contamination is lower than flask culture. There are multiple reports describing reduction of expansion rate once cells are transferred from a small flask to a larger disposable bag (Siegler et al., 2010; Sutlu et al., 2010).

In order to avoid frequent media exchange during the culture, a cell culture flask with gas permeable membrane was developed, named G-Rex. The G-Rex looks like a regular media bottle, but the membrane at the bottom for exchanging carbon dioxide and transfer oxygen from external environment. If cells are cultured in a T flask with high volume of cell culture media, cells will not be able to receive enough oxygen from outside, and will eventually die due to hypoxia. The membrane is designed to supply oxygen for cells settled at the bottom. Now with G-Rex, it is usually filled with media to the neck of the body, and is kept under culture condition without changing the media for more than 10 days without changing media. G-Rex was able to yield higher cell number compared to cell culture bags (Lapteva et al., 2012). Although there is less risk of contamination, the risk from manual handling still exists. The size of the G-Rex is also a concern that the surface area at the bottom is still not enough to produce a large number of cells.

Automated systems can be used to culture NK cells without human intervention. It increases accuracy of liquid handling and decreases the risk of contamination. The initial capital cost for the automated system is larger than the cost of manual cell handling. However, due to lower cost of human manpower, the cost of running the system in a long term will be lower. First generation of automated system is using

a bioreactor. Both stainless steel and disposable bioreactors showed their capability culturing NK cells for expansion. The bioreactors are capable of controlling temperature, agitation, dissolved oxygen level, and supplying nutrient feed if necessary. However, setting up the reactor and transferring cells in and out still need human intervention, which may pose a risk of contamination because NK cells need to be isolated from blood. In addition, additional steps, such as washing the cells after cultivation and concentrate the cell density may be necessary after cell expansion that are difficult to be performed inside the bioreactor.

In an effort to develop an automated system that can handle multiple unit operations in a single machine, CliniMACS Cell Separation system provides a closed system handling steps including isolation from blood, washing, labeling with antibody followed by separation, expansion, volume reduction for higher cell concentration, and final buffer formulation prior to cryopreservation (Apel et al., 2013).

2.3 NK Cell Culture: Autologous Feeder Cells

Cytokines play important roles during maturation and expansion of NK cells. However, the degree of expansion caused by adding cytokines to the culture is not high enough that it is difficult to meet the demand of NK cells for clinical and commercial use. By adding autologous feeder cells from the patient, it triggers better expansion compared to culture proliferating NK cells alone. In Peripheral Blood Mononuclear Cells, there are T cells, B cells, NK cell and monocytes. T cells have a distinct marker CD3, B cells have CD19, and monocytes have CD14. For

instance, CD19+ monocytes enhance NK cell expansion by direct cell to cell contact, and by secreting molecules that triggers NK cell expansion (J. S. Miller, Oelkers, Verfaillie, & McGlave, 1992; Pierson, Miller, Verfaillie, McGlave, & Hu, 1994).

While autologous feeder cells are cultured with NK cells, a combination of cytokines and antibodies, such as IL-2, IL-15, OKT-3 (Anti-CD3 Antibody), are added to promote a better growth. OKT-3 is known to activate T cells within the autologous cell population, and the activated T cells stimulate NK cells to expand. A number of reports indicated that autologous feeder cells yield better expansion of NK cells while the number of T cells in the culture also expand. At the end of the culture, only 30-60% population was NK cells, and the rest was mostly T cells (Barkholt et al., 2009; Carlens et al., 2001; Geller et al., 2011; Sutlu et al., 2010).

In the effort to avoid growing population of T cells, autologous feeder cells can be irradiated. This will result in very small population of T cells at the end of expansion. The benefit of irradiation is not only preventing unwanted cells growing, but also inducing stress-induced surface markers, such as UL Binding Protein. Activating receptor NKG2D recognizes UL Binding Protein on the surface of the feeder cells. By recognizing the stress-induced markers, NK cells are better activated (Ahn et al., 2013).

2.4 NK Cell Culture: Allogeneic Feeder Cells

One advantage that allogenic feeder cells carry is an ease of having off the shelf stock of the feeder cells. Because the feeder cells are not coming from the patient directly, Peripheral Blood Mononuclear Cells (PBMCs) from other donors can be used as well as established cell lines can be developed. In the previous section, autologous PBMCs were culture with NK cells to increase the proliferative capacity. When allogeneic PBMCs were cultured with NK cells, it yielded around 300-fold expansion compared to 169-fold expansion when autologous PBMCs were utilized (Kim et al., 2013).

While PBMCs give NK cells signals for proliferation either in direct or indirect manner, cell lines such as K562 and Epstein-Barr virus infected cells give much higher proliferative signals compared to PBMCs. The advantage of stimulation with genetically modified K562 is not just higher cell numbers, but also higher cytotoxicity compared to unstimulated NK cells.

K562 is a leukemia cell line that is well known to be a target cell for lysis by NK cells. During the course of lysis of K562, NK cells become activated by upregulating surface receptors. K562 cell lines had been genetically modified to express certain molecules that typically do not exist on the surface of NK cells. The molecules are also known to stimulate and expand T cells.

There are different combinations of molecules that were transduced on K562, including CD137L, MICA, 4-1BB Ligand, IL-15, IL-21. Because gamma chain cytokines are also known to promote NK cell expansion, IL-15 and IL-21 were

mixed with media in soluble form, but they were able to be expressed on K562 to stimulate NK cells at a higher level.

Fujisaki transduced K562 cell lines with constructs encoding membrane bound form of IL-15, CD8α, and 4-1BB ligand. Because K562 expands faster than NK cells, K562 needs to be irradiated prior to co-culture. During 7 day co-culture, the number of NK cells expanded from 5.1 to 86.6 fold (median 21.6 fold) compared to the number of NK cell on Day 0 (Fujisaki et al., 2009). All cells undergo senescence after a prolonged culture period. NK cells showed slower growth rate when they were cultured with K562 with membrane bound IL-15.

Denman showed that NK cells co-cultured with K562 membrane bound IL-21 does not show senescence after 60 days of culture. The genetically modified K562 were produced by retroviral transduction with CD64 (FcγRI), CD86 (B7-2), CD137L (4-1BB), and truncated CD19 with membrane bound IL-21 using *Sleeping Beauty* transposon. He showed on average 47,967-fold expansion after 21 days of co-culture with genetically modified K562. Denmen stated that the reason why membrane bound IL-21 performed superior compared to membrane bound IL-15 was due to the length of telomere of NK cells with K562 membrane bound IL-21 cells was maintained 10% longer than the length of telomere before stimulation on Day 0 while the length of telomere of NK cell cultured with K562 membrane bound IL-15 showed 10% shorter compared to Day 0 (Denman et al., 2012).

2.5 Effect of Cytokines on NK Cell Activation and Expansion (IL-2, IL-15, IL-21)

There is an array of surface receptors on the surface of cells. Cytokines bind to those receptors, and regulate survival, activation, expansion of the cells.

Interleukin-2 (IL-2) binds to IL-2R (Letter 'R' denotes receptor), and activates NK cells. It was originally identified as a T cell growth factor. However, it also stimulates NK cells by upregulation of natural cytotoxicity receptors (NCRs) and NKG2D. Also, a proportion of KIR+ population increased over KIR- population (Huenecke et al., 2010). After activation of NK cells by IL-2, they showed higher cytotoxicity against K562.

While IL-2 is better known for its activation characteristics of NK cells, IL-15 has received its popularity for expansion of NK cells. IL-15 also belongs to gamma chain cytokines. Similar to IL-2, it was first identified a T cell growth factor. Later, it was also found that the *in vitro* effect of IL-15 is comparable to IL-2 because the signaling by both IL-2 and IL-15 occurs at the same location called IL-2/15 Rβ and γ_c subunits. However, in vivo effect of IL-2 and IL-15 are different (Bamford et al., 1994; Carson et al., 1994; Grabstein et al., 1994). Besides its effect of activating of NK cells, IL-15 causes functional exhaustion of the cells as it alters *in vivo* activity of the NK cells (Felices et al., 2016). Therefore, proper dose and duration of cultivating NK cells with IL-15 should be carefully considered to avoid the exhaustion effect.

IL-21 is another member of gamma chain cytokine that is known to enhance expansion of NK cells. It is produced by CD4+ T cells and has effects on different types of cells. When NK cells are cultured with media containing IL-21, effector function of NK cell is enhanced showing higher cytotoxicity and ADCC responses (McMichael et al., 2017).

3 METHODS

3.1 ISOLATION OF PERIPHERAL BLOOD MONONUCLEAR CELLS FROM BLOOD

Concentrated blood samples are obtained from Memorial Blood Centers in Minneapolis, MN using a blood processing system such as TRIMA ACCEL blood component centrifuge manufactured by Terumo BCT, Inc. The volume of concentrated blood in the blood cell collection device is approximately 10 mL. Dilute the concentrated blood with 50 mL of Phosphate Buffered Saline (PBS, Corning 21-040-CV). Use a syringe to purge leftover blood in the blood cell collection device. In a 50 mL falcon tube (Falcon 352098), aliquot 20 mL of Ficoll-Paque PREMIUM density gradient media (GE Healthcare 17-5442-03), then gently fill up the tube with 30 mL of the diluted blood. The tubes can be centrifuged at 400 g for 30 minutes with no brake. From the top of the tube, there will be a layer of plasma, mononuclear cells, Ficoll-Paque media, and a combination of granulocytes and erythrocytes.

Remove upper half of plasma. Then, collect the lower half of plasma and a thin layer of mononuclear cells. Centrifugate the collected mononuclear cells at 400 g for 5 minutes. Remove the supernatant and add 20 mL of PBS with 2% Human AB Serum and 2% EDTA. Count the number of cells accordingly.

3.2 ISOLATION OF NK CELLS FROM PBMC

Wash the PBMC twice using PBS with 2% Human AB Serum and 2% EDTA. Adjust the cell concentration to 1 x 10^8 cells/mL, and transfer the cells into a 14 mL polystyrene round-bottom tube (Corning 352051). Add Selection Cocktail to the tube at 100 µL/mL of the sample from each of EasySep Human CD3 Positive Selection Kit II (STEMCELL Technologies 17851) and EasySep Human CD19 Positive Selection Kit II (STEMCELL Technologies 17854). Mix and incubate at room temperature for 3 minutes. Vortex RapidSpheres magnetic beads for 30 seconds before adding to the tube. Add magnetic beads to the tube at 100 µL/mL of the sample in the tube. Mix and incubate at room temperature for 3 minutes. If the volume of sample is less than 2 mL, top up with PBS with 2% Human AB Serum and 2% EDTA to 3 mL level of the tube. If the volume of sample is more than 2 mL, top to with PBS with 2% Human AB Serum and 2% EDTA to 10 mL level of the tube. Place the tube into The Big and Easy magnet (STEMCELL Technologies 18001) at room temperature for 3 minutes. Pick up the magnet, and in one continuous motion invert the magnet and tube, pouring off the supernatant. Remove the tube from the magnet; this tube contains the isolated cells. Repeat the magnetic isolation twice more for better purity of the sample. Count the number of cells at the end. The sample includes NK cells and monocytes.

EasySep Human NK Cell Enrichment Kit (STEMCELL Technologies 19055) can be used for a pure population of NK cells without monocytes from PBMC following the same step described above.

3.3 CULTIVATION OF NK CELLS

500 mL of NK cell culture media contains 300 mL of Dulbecco's Modified Eagle Medium (DMEM) with 25mM HEPES, 4.5 g/L glucose, and L-glutamine, without sodium pyruvate (Corning 10-027), 150 mL of Ham's F-12 medium (Corning 10-080), 50 mL Heat-inactivated Human AB Serum (Valley Biomedical HP 1022HI), 5 mL Penicillin and Streptomycin (Gibco 15140), 20 uM 2-Mercaptoethanol (Sigma M7522), 50 uM Ethanolamine (Sigma E0135), 10 ug/mL Ascorbic Acid (Sigma A4544), and 1.6 ng/mL Sodium Selenite (Sigma S5261).

Genetically modified K562 cells were obtained from Fate Therapeutics. Upon collection of either CD3, CD19 depleted or CD56 enriched NK cells, 8 x 10^6 cells were placed in a T-75 flask (Corning 353136) with 40 mL of media. 1.6 x 10^7 genetically modified K562 cells were added to the T-75 flask. Half-volume media changes are performed on day 3 and 5 without diluting the cells. On day 7, NK cells are diluted to 5 x 10^6 cells, and genetically modified K562 cells are added at a 1:1 ratio for re-stimulation. From day 7 onwards, full-volume media changes were performed every 2 or 3 days while diluting the NK cells to 1 x 10^7 cells. Re-stimulation by genetically modified K562 cells were performed every 7 days.

Cell counts were performed using Tripan-Blue Dye Exclusion method. Countess II Automated Cell Counter (Thermo Fisher Scientific) was used to determine the number of cells in a single slide containing 5 µL of Trypan-Blue solution, and 5 µL of cell culture sample.

3.4 SURFACE ANTIBODY STAINING FOR FLOW CYTOMETRY

5 x 10^5 cells were obtained from the culture. Wash the cells with PBS before starting the procedure. Place cells into a 5 mL polystyrene round-bottom tube (Falcon 352052).

Following antibodies were subsequently added to stain the cells.

Table 1: List of Antibodies for Flow Cytometry

Target	Color	Manufacturer	Cat. No.
CD366	Brilliant Violet 421	Biolegend	345008
CD11a	FITC	Biolegend	301206
CD96	PE/Dazzle 594	Biolegend	338414
CD85j (ILT2)	Per/CP Cy 5.5	Biolegend	333714
TIGIT	APC	R&D Systems	FAB7898A
CD45RA	Brilliant Violet 421	Biolegend	304130
CD16	FITC	Biolegend	302006
CD2	Brilliant Violet 510	Biolegend	300218
CD44	Brilliant Violet 510	BD	563029
CD164	FITC	Biolegend	324806
CD52	PE/Dazzle 594	Biolegend	316014
CD56	PE/Cy7	Biolegend	92189
CD16	Brilliant Violet 421	Biolegend	302038
CD3	Brilliant Violet 785	Biolegend	93380
IFN-g	Brilliant Violet 650	Biolegend	93705
NKG2D	Brilliant Violet 510	Biolegend	320816
CD117	Brilliant Violet 711	Biolegend	313230
KIR2DL1 (CD158)	FITC	Biolegend	339504
KIR3DL1 (CD158j)	FITC	Biolegend	312706
KIR2DL2 (CD158b)	FITC	Biolegend	312604
CD319	PE/Dazzle 594	Biolegend	331812
CD62L	Per/Cp Cy 5.5	Biolegend	304824
CD107a	Per/Cp Cy 5.5	Biolegend	92580
NKG2A (CD159a)	PE	Beckman Coulter	IM3291U
CD81	Per/Cp Cy 5.5	Biolegend	349508
DNAM-1 (CD226)	Per/Cp Cy 5.5	Biolegend	338314
CD44	Brilliant Violet 510	BD	563029

Because the number of colors that can fit into a single panel is limited, antibodies were grouped into three different panels.

Table 2: List of Markers Used for Three Flow Cytometry Panels

Color	Panel 1	Panel 2	Panel 3
PE-Cy7	CD56	CD56	CD56
APC-Cy7	Livedead	Livedead	Livedead
BV605	CD57	CD57	CD57
BV786	CD3	CD3	CD3
FITC	3KIRs	LFA-1	CD164
PE	NKp30	NKG2C	NKG2A
PE-CF594	CD319	CD96	CD52
PerCP-Cy 5.5	CD62L	ILT2	CD81
APC	N/A	TIGIT	CD45RO
Alexa Flour 700	2B4	N/A	N/A
BV421	CD16	TIM-3	CD45RA
BV510	NKG2D	CD2	CD44
BV711	CD117	N/A	N/A

The shaded region in the table represents that are in common among all three panels. Those were used to gate NK cell population from the sample, and determine the level of maturity by CD57.

In case of complex antibody staining that consists of multiple colors, the antibodies need to be mixed with BD Brilliant Stain Buffer (BD 563794) to prevent antibodies aggregate each other. The tube is incubated at 4 °C for 30 minutes.

3.5 SPADE ANALYSIS

SPADE (Spanning-tree Progression Analysis of Density-normalized Events) is a method to identify specific subset of cell populations using data files obtained from multidimensional flow cytometry analysis. Flow cytometry data consists of the expression intensity of every single cell processed through the cytometer. SPADE clusters all cells in the data into a defined number of ‘nodes’ and visualize the nodes into a tree like structure. Due to the nature of cytometry, SPADE can be used for both flow cytometry and mass cytometry.

3.5.1 Establishment of SPADE Analysis Methodology

One of the biggest advantages of the SPADE is the ability to visualize multi-dimensional data into a single plane. Because there are different phenotypes present in every single sample, it is important to combine the data into one single file so that the combined dataset can present all the phenotypes possible throughout the co-cultivation.

NK cells cultivated from five donors were used to collect the data. A publicly available tool, Cytobank (Kotecha, Krutzik, & Irish, 2010), was used to analyze the data using SPADE. Cytobank provides a tool to concatenate multiple FCS files into one single FCS file. All individual FCS files that are concatenated must have the same markers and channels aligned to avoid errors during the concatenation. (Figure 1)

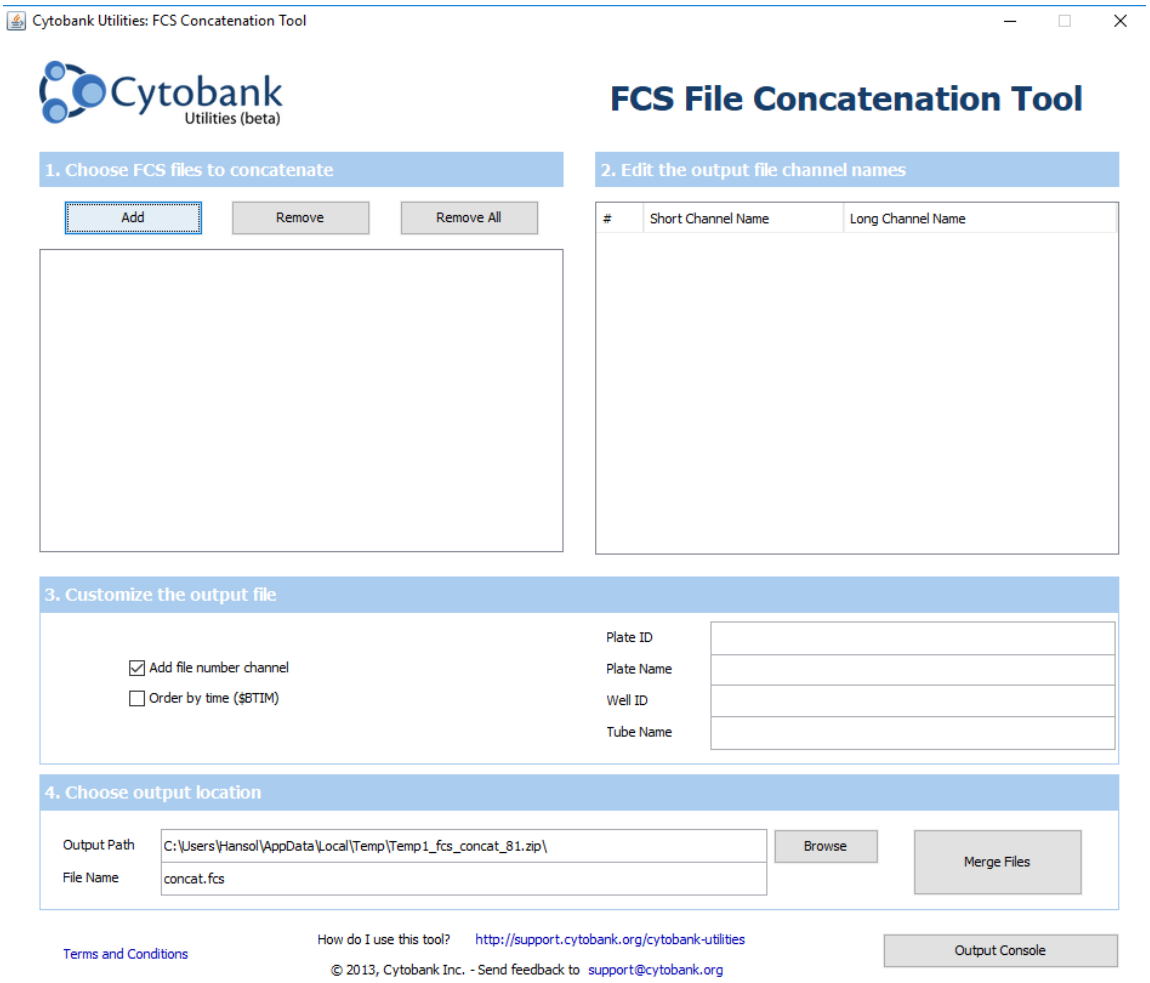

Figure 1: Cytobank File Concatenation Tool

When the data was visualized using histograms, all five donors showed similar expression although the degree of activation by co-cultivation varied depending on the donor.

Each node represents a group of cells showing similar phenotype expression intensity. Defining the correct number of nodes will bring the best results. By setting the number lower, the shape of the tree will be simplified. However, it will also compromise the chance to detect a rare or subtle population. This is so called "underclustering". On the other hand, setting the number of the nodes higher than

needed, so called “overclustering”, will be clustering the data at a high definition, but will require more time to analyze and form a bubble that contains multiple nodes showing similar characteristics. In order to define the right number of nodes for the dataset, a number of SPADE analysis were tested that gave the smallest node that contained less than 0.1% of the total population. When 150 nodes SPADE analysis was created, the smallest node contained 0.08% of the total population, which satisfied the criteria of less than 0.1%.

Nodes that had similar phenotypes were manually clustered based on pre-defined criteria, named ‘bubble’. By using this method, proportion of certain phenotypes of interest can be easily identified and visualized among multiple donor or patient.

Once all the bubbles were formed, median values of each node were calculated. Cytobank used the median values to show the intensity of each node. The median value right after clustering was presented in a linear scale. Then, the linear median values were transformed into a new scale called ‘arcsinh’.

The flow cytometer equipment used for this experiment (BD LSR II) used Log10 scale to visualize the data in two-dimension, and also biexponential scaling to avoid pitfall of failure to display data near zero. In cytobank, it supports log-like scale called ‘arcsinh’ to allow for configuration of the linear region around zero through adjustment of the cofactor.

By looking at the histograms, and overlaying them to check the difference between the donor, initial conclusion was the donor variation exists, but it should not affect the analysis too much. In order to verify the effect of donor variation, a dataset

contained all five donors, and another dataset contained only one donor flow cytometry data files were compared.

For the analysis of all five donors concatenated, the dataset contained all files listed in Table 3, plus one concatenated file. For the analysis of one donor, the dataset contained files belong to only one donor cultivated using one type of feeder cells.

Table 3: List of Samples Tested

Donor ID	Feeder Type	Sampling Day
SLR833	Native K562	0
		7
		14
	K562.mbIL10	0
		7
		14
	K562.mbIL15	0
		7
		14
	K562.mbIL21	0
		7
		14
SLR842	Native K562	0
		7
		14
	K562.mbIL10	0
		7
		14
	K562.mbIL15	0
		7
		14
	K562.mbIL21	0
		7
		14
SLR843	Native K562	0
		7
		14
	K562.mbIL10	0
		7
		14

Donor ID	Feeder Type	Sampling Day
	K562.mbIL15	0
		7
		14
	K562.mbIL21	0
		7
		14
SLR856	Native K562	0
		7
		14
	K562.mbIL10	0
		7
		14
	K562.mbIL15	0
		7
		14
	K562.mbIL21	0
		7
		14
SLR859	Native K562	0
		7
		14
	K562.mbIL10	0
		7
		14
	K562.mbIL15	0
		7
		14
	K562.mbIL21	0
		7
		14
NOTE: All Day 0 samples are tested before starting the co-culture. This means there will be only one Day 0 sample file available for each donor even though the table lists as a separate file.		

3.5.2 Comparison between 5-donor and 1-donor Concatenated Dataset

In order to make sure five-donor data concatenation did not have much effect on the analysis due to donor to donor variation, proportion of pre-defined phenotypes were compared between the two datasets to show the comparability. Among the three panels, Panel 1 was chosen, and also three donors among five to compare the proportion of certain phenotypes.

There were four phenotypes defined by looking at the most dominant phenotype shown on each sampling day. From Panel 1, there were 9 markers available (3KIR, NKp30, CD319, CD62L, 2B4, CD16, NKG2D, CD117 and CD57) while excluding common markers across the three panel to gate the NK cells. Only 4 out of 9 markers showed clear separation of positive and negative phenotype when they were visualized in histogram (Figure 2).

a)

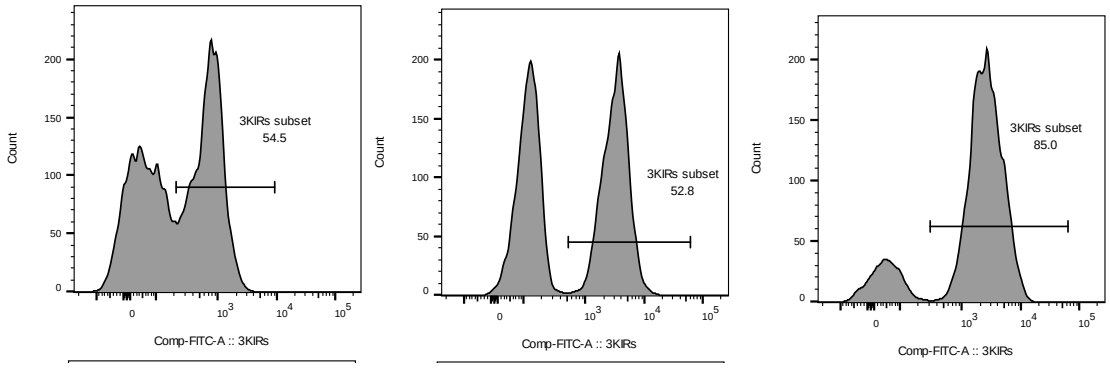
Count
3KIRs subset
54.5
Comp-FITC-A :: 3KIRs
3KIRs subset
52.8
Comp-FITC-A :: 3KIRs
3KIRs subset
85.0
Comp-FITC-A :: 3KIRs

b)

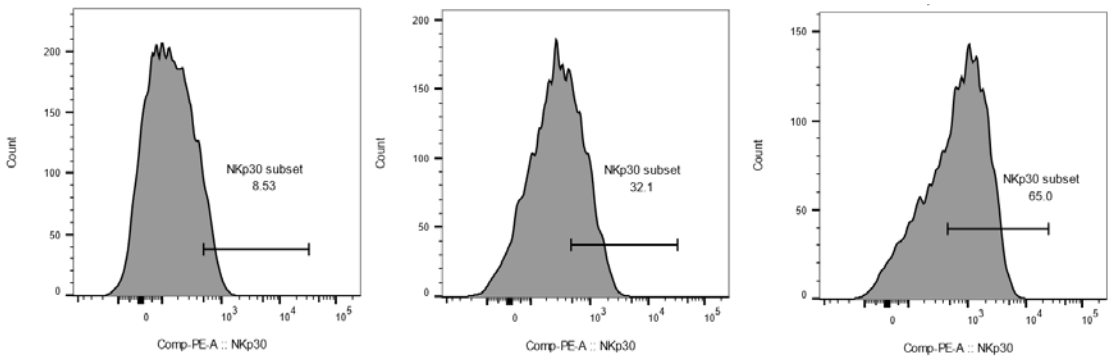
Count
NKp30 subset
8.53
Comp-PE-A :: NKp30
NKp30 subset
32.1
Comp-PE-A :: NKp30
NKp30 subset
65.0
Comp-PE-A :: NKp30

c)

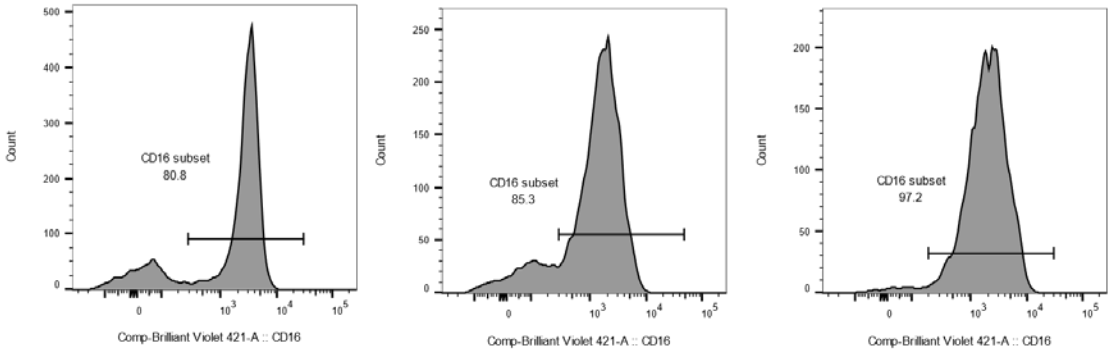
Count
CD16 subset
80.8
Comp-Brilliant Violet 421-A :: CD16
CD16 subset
85.3
Comp-Brilliant Violet 421-A :: CD16
CD16 subset
97.2
Comp-Brilliant Violet 421-A :: CD16

d)

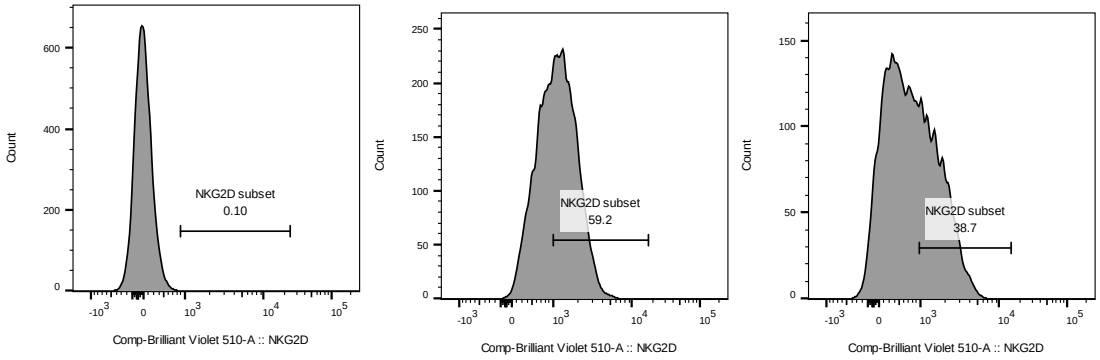

Figure 2: Flow Cytometry Intensity Histogram for 3KIRs, NKp30, CD16, NKG2D

(a) Flow Cytometry Intensity Histogram for 3KIRs. Day 0, 7, 14 (Left to Right)

(b) Flow Cytometry Intensity Histogram for NKp30. Day 0, 7, 14 (Left to Right)

(a) Flow Cytometry Intensity Histogram for CD16. Day 0, 7, 14 (Left to Right)

(a) Flow Cytometry Intensity Histogram for NKG2D. Day 0, 7, 14 (Left to Right)

Other markers did not show clear separation between positive and negative phenotype. Therefore, all nine markers were clustered by SPADE, but only 4 of which had shown clear separation were annotated.

For the four markers annotated, values that separates phenotypes were recorded in linear scale. Because cytobank used an arcsinh transformation, the linear values obtained from histogram visualization were transformed in excel by '=ASINH(value/cofactor)' command. Note that the value of cofactor was obtained from scale setting of each panel.

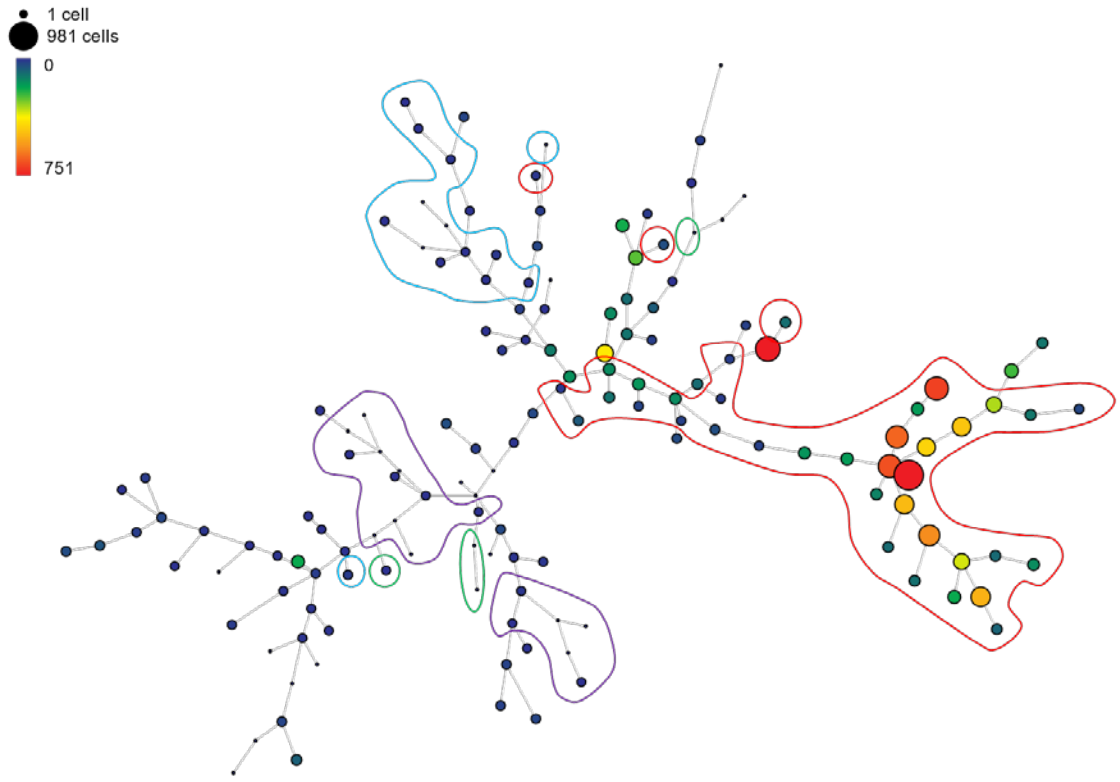

Figure 3: SPADE Figure from Donor SLR833, Day 0. Generated from Five Donor Concatented Dataset

Red bubbles indicate 3KIRs-NKp30^{-}CD16^{+}NKG2D^{-}, which were dominant on Day 0. Green bubbles indicate 3KIRs^{+}NKp30^{-}CD16^{+}NKG2D^{+}, and blue bubbles indicate 3KIRs^{-}NKp30^{+}CD16^{+}NKG2D^{+}, which were dominant on Day 7. Purple bubbles indicate 3KIRs^{+}NKp30^{+}CD16^{+}NKG2D^{+}, which were partially dominant on Day 14, and also the most idealistic phenotype.

Based on the gating values defined, four different pre-defined phenotypes that are dominant on Day 0, 7, and 14 were grouped into bubbles.

After defining the bubbles of each phenotype from a SPADE figure that contains all five-donor data, the exact same bubbles were used to measure proportion of each phenotype present on each donor and each day. Figure 3, Figure 4, Figure 5 show only one donor, and how the proportion changes over time.

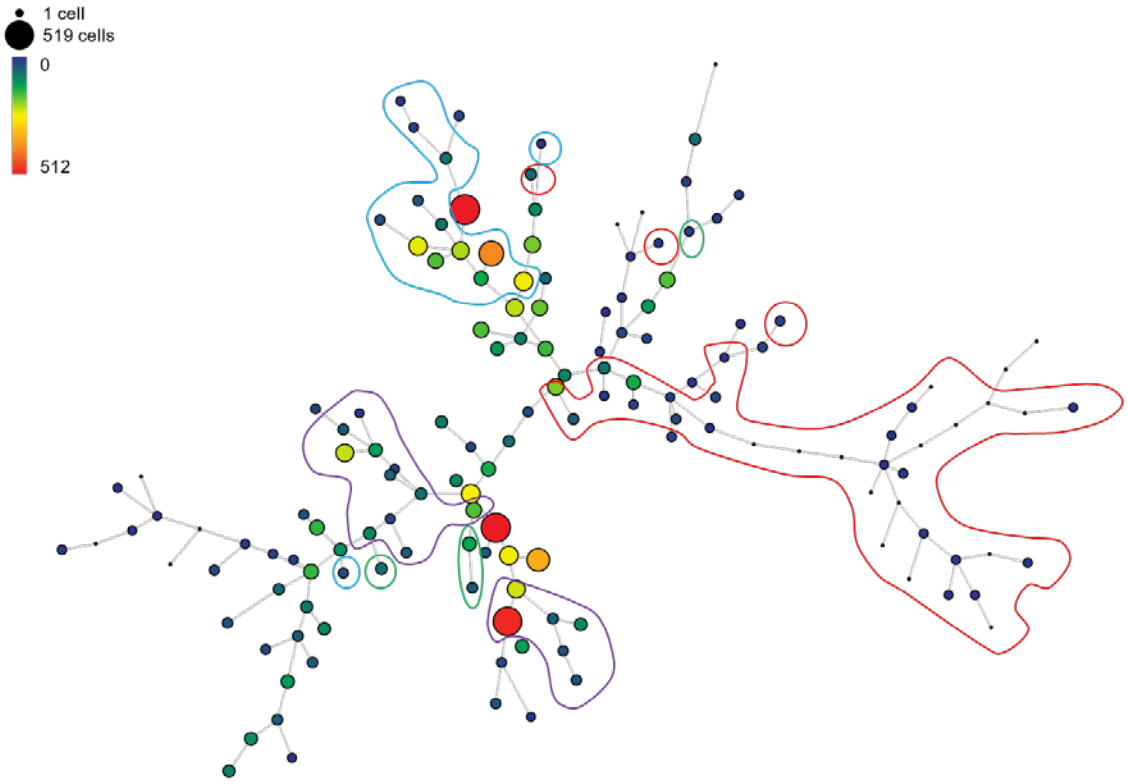

Figure 4: SPADE Figure from Donor SLR833, Day 7. Generated from Five Donor Concatenated Dataset

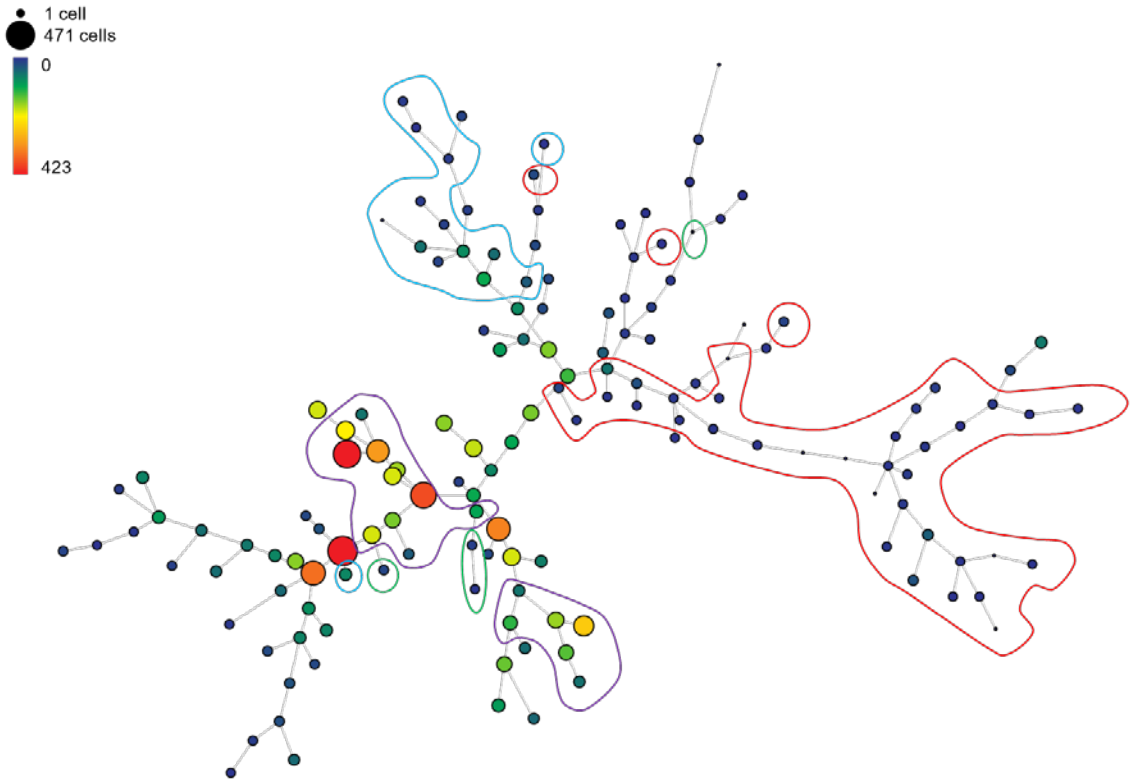

Figure 5: SPADE Figure from Donor SLR833, Day 14. Generated from Five Donor Concatenated Dataset

By calculating the number of cells captured within a bubble, proportions of each phenotype in the five-donor concatenated dataset were calculated. In order to compare the characteristics of each bubble, the average values of each bubble were also calculated.

Table 4: Proportion of pre-defined phenotypes from five donor concatenated dataset

Proportion (%)	Day 0				Day 7				Day 14			
Donor / Phenotype	**A**	**B**	**C**	**D**	**A**	**B**	**C**	**D**	**A**	**B**	**C**	**D**
SLR 833	70.08	0.01	0.39	0.19	6.53	5.80	16.41	19.36	4.19	1.84	5.53	31.95
SLR 842	72.45	0.22	0.74	0.54	4.88	3.26	41.77	23.30	12.05	1.51	8.41	18.20
SLR 856	51.91	0.08	0.43	0.24	35.92	3.39	3.38	4.74	2.55	0.53	18.30	25.74

A represents 3KIRs-NKp30^{-}CD16^{+}NKG2D^{-}. B represents 3KIRs^{+}NKp30^{-}CD16^{+}NKG2D^{+}. C represents 3KIRs^{-} NKp30^{+}CD16^{+}NKG2D^{+}. D represents 3KIRs^{+}NKp30-CD16^{+}NKG2D^{+}.

Table 5: Average intensity of each bubble from five-donor concatenated dataset

Average Intensity	3KIRs	NKp30	CD16	NKG2D	CD319	CD62L	2B4	CD57	CD117
A	1.31	1.31	2.27	1.65	0.37	0.78	1.00	1.64	0.28
B	4.65	1.52	2.63	3.53	0.90	0.18	1.41	0.90	0.56
C	1.30	3.28	2.29	3.73	1.06	0.42	1.40	0.33	0.59
D	4.67	3.22	2.55	3.67	1.08	0.56	1.56	1.43	0.54

After determining the characteristics of five donor concatenated dataset, the same procedure was repeated for one donor dataset. The same procedure was repeated for the three donors to identify changes in proportion among different donors. Figure 6, Figure 7, Figure 8will show only the SPADE figures for donor SLR 833, but the Table 6 and Table 7include all calculations to determine the comparability.

After all the characteristics from individual donor data were calculated, data between five-donor and one-donor datasets were compared. It was concluded that proportions of phenotypes measured from both dataset showed similarity to negate the variation between the two datasets.

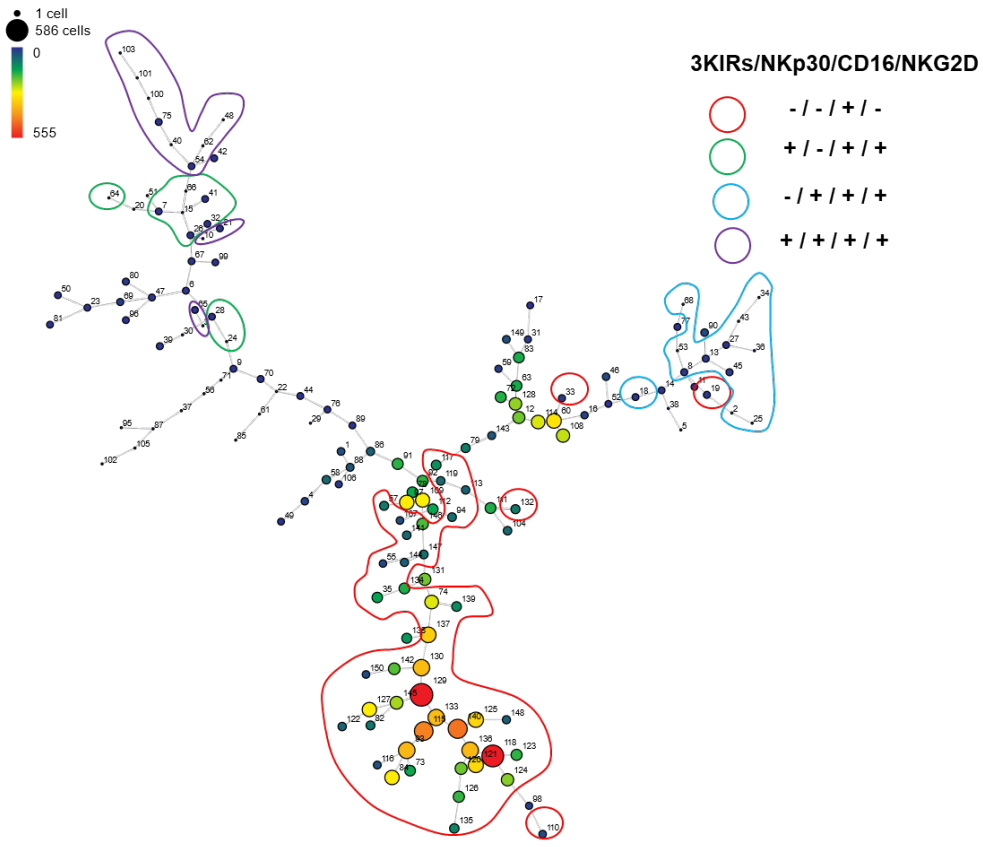

Figure 6: SPADE Figure from Donor SLR833, Day 0. Generated from One Donor Concatenated Dataset

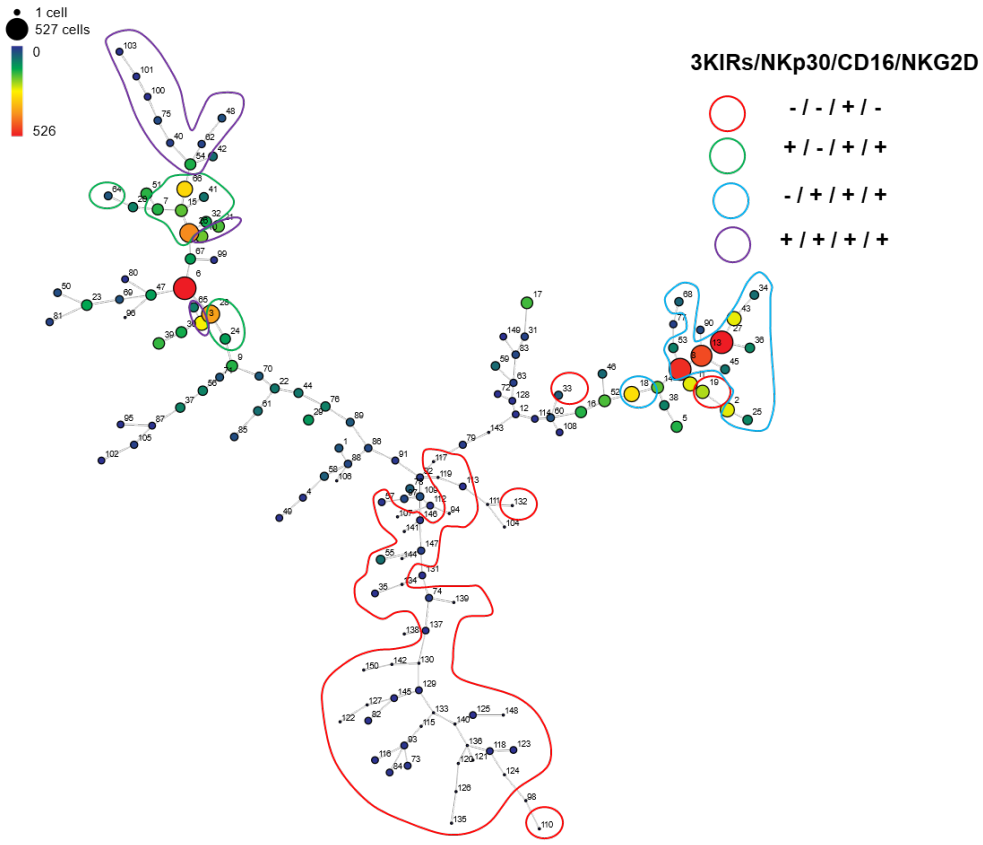

Figure 7: SPADE Figure from Donor SLR833, Day 7. Generated from One Donor Concatenated Dataset

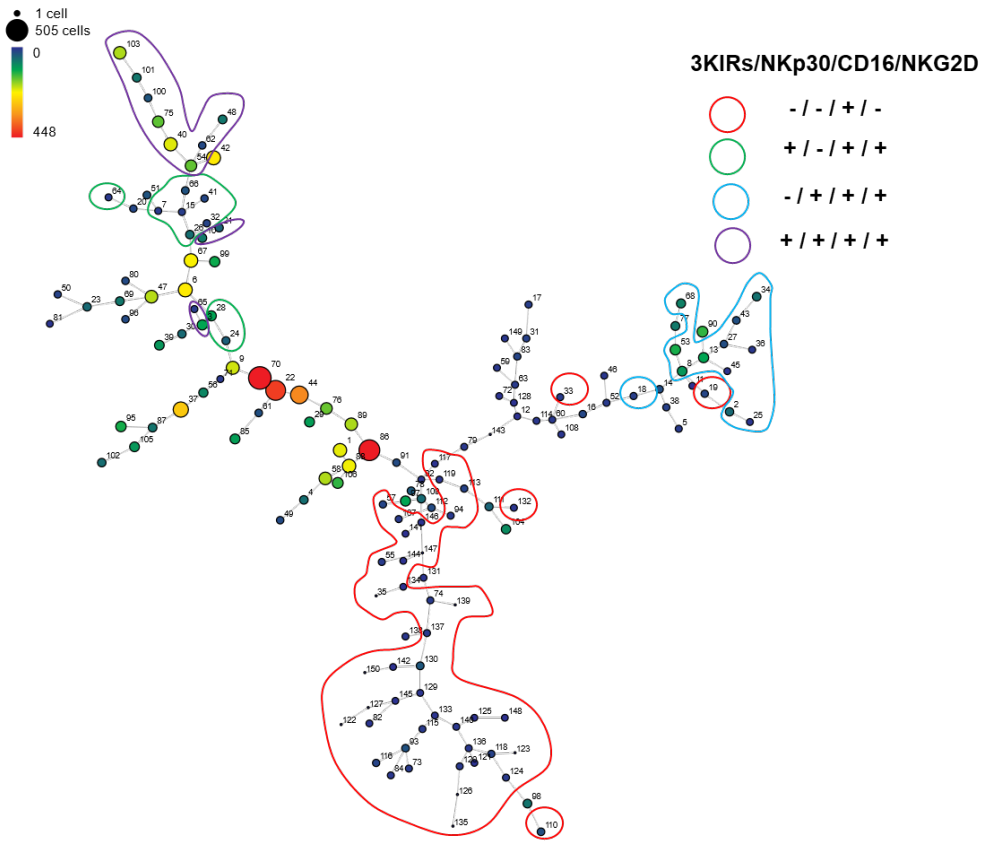

Figure 8: SPADE Figure from Donor SLR833, Day 14. Generated from One Donor Concatenated Dataset

Table 6: Proportion of pre-defined phenotypes from one donor concatenated dataset

Proportion (%)	Day 0				Day 7				Day 14			
Donor / Phenotype	**A**	**B**	**C**	**D**	**A**	**B**	**C**	**D**	**A**	**B**	**C**	**D**
SLR 833	67.09	0.05	0.29	0.10	4.01	16.75	28.07	13.27	3.98	3.33	7.13	31.03
SLR 842	76.73	0.03	0.20	0.18	4.10	1.09	49.55	27.54	19.26	0.87	8.77	21.08
SLR 856	67.24	0.12	0.13	0.07	42.69	2.31	1.38	2.45	4.74	0.26	19.09	25.77

A represents 3KIRs-NKp30^{-}CD16^{+}NKG2D^{-}. B represents 3KIRs^{+}NKp30^{-}CD16^{+}NKG2D^{+}.

C represents 3KIRs^{-}NKp30^{+}CD16^{+}NKG2D^{+}. D represents 3KIRs^{+}NKp30-CD16^{+}NKG2D^{+}

Each bubble consists of multiple nodes that has different median values. Weighted median was calculated for each bubble to determine the characteristics of each bubble.

Table 7: Average intensity of each bubble from one donor concatenated dataset.

Donor	Average Intensity	3KIRs	NKp30	CD16	NKG2D	CD319	CD62L	2B4	CD57	CD117
SLR 833	A	2.35	1.38	2.97	0.86	0.25	0.62	0.83	4.23	0.17
	B	4.55	1.32	2.34	3.39	1.03	0.42	1.43	2.91	0.45
	C	1.27	2.83	2.48	3.60	1.03	0.57	1.43	0.40	1.01
	D	4.56	3.27	2.90	3.66	1.13	0.42	1.72	1.74	0.68
SLR 842	A	1.58	1.61	2.80	1.25	0.40	0.99	0.99	2.13	0.24
	B	4.12	1.20	2.42	3.39	0.72	0.34	1.44	1.65	0.09
	C	1.31	3.18	2.93	4.16	1.21	0.62	1.48	0.55	0.76
	D	4.45	3.28	2.92	3.88	1.13	0.40	1.64	0.72	0.76
SLR 856	A	1.13	1.44	1.91	1.54	0.35	1.23	1.00	1.19	0.23
	B	4.72	1.11	2.41	3.58	1.01	0.91	1.68	0.57	1.19
	C	0.86	3.71	2.20	3.71	1.09	0.41	1.52	0.00	0.73
	D	4.70	3.59	2.42	3.62	1.00	0.67	1.64	0.18	0.64

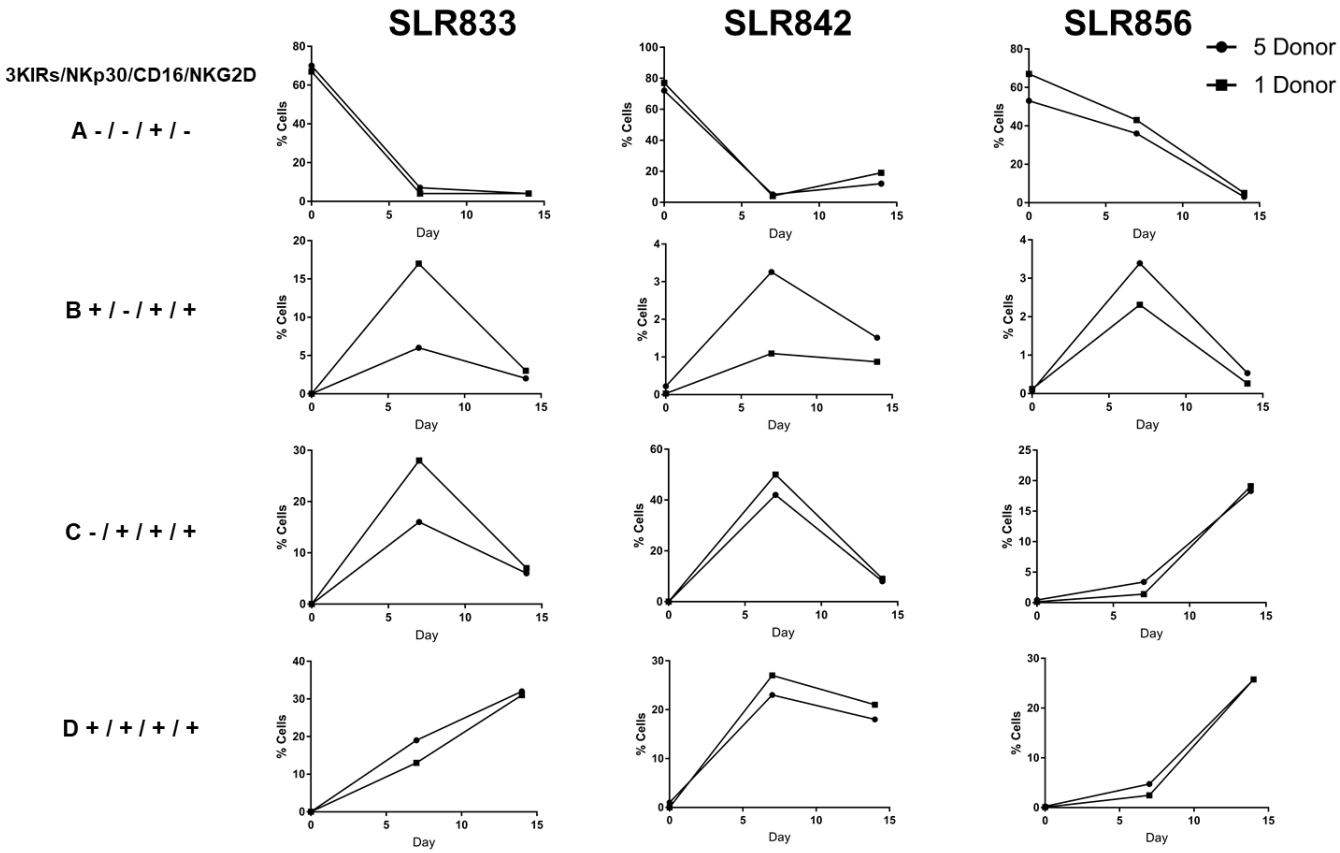

Figure 9: Comparison between five-donor concatenated and one-donor concatenated for each pre-defined phenotype across 3 donors.

3.6 Glucose Consumption Measurement

Glucose consumption by NK cells was measured by taking supernatant samples from the culture every 2-3 days during the cultivation. In order to quantify the amount of glucose in the supernatant, Infinity Glucose Hexokinase Liquid Stable Reagent (Thermo Scientific TR15421) was used. In a 96 well plate, 2 µL of sample was mixed with 300 µL of the reagent. The mixture was kept in 37 °C for 30 minutes for incubation, and was measured for absorbance at 340 nm using Tecan Infinite 200 PRO plate reader. The actual amount of glucose in the solution was calculated by fitting the absorbance value into a pre-determined slope that measured known concentration of glucose solution. All measurements were done in triplicate to ensure consistency of the measurements.

3.7 Oxygen Consumption Measurement

Oxygen consumption by NK cells was measured using NeoFox Phase Fluorometer to quantify the amount of dissolved oxygen in the cell culture media. In order to measure the level of dissolved oxygen changing over time, the probe was calibrated per the instructions of the fluorometer. During the cultivation, certain number of cell was sampled, and was centrifuged to lower the volume so that cell density can be increased. Centrifuged cells were placed into a 1.8 mL HPLC vial (Agilent Technologies), and the media was filled up to 1 mL. In order to avoid gas transfer between ambient air and the liquid, 200 µL of paraffin oil (EMD Millipore) was place on top of the solution.

After placing a blue cap with septa (Agilent Technologies), the septa was punctured with the measurement probe, and placed into a waterbath that was set to 37.0 °C.

Initial and final concentration of dissolved oxygen was measured, and also the slope was plotted to ensure the oxygen level dropped in a linear fashion.

4 RESULTS

4.1 LIMITATION OF NK CELL CULTIVATION WITHOUT FEEDER CELLS

NK cells isolated from three donors and enriched by magnetic bead isolation as described in Materials and Methods were inoculated into 24 well plate at 1 x 10^6 cells/mL. The medium was supplemented with a gamma chain cytokine IL-15 at 50 IU/mL. Complete media replenishment was performed on Day 7. All donors showed only limited growth over 14 days. The final cell concentration was 2.35, 2.27, 1.57 x 10^6 cells/mL respectively.

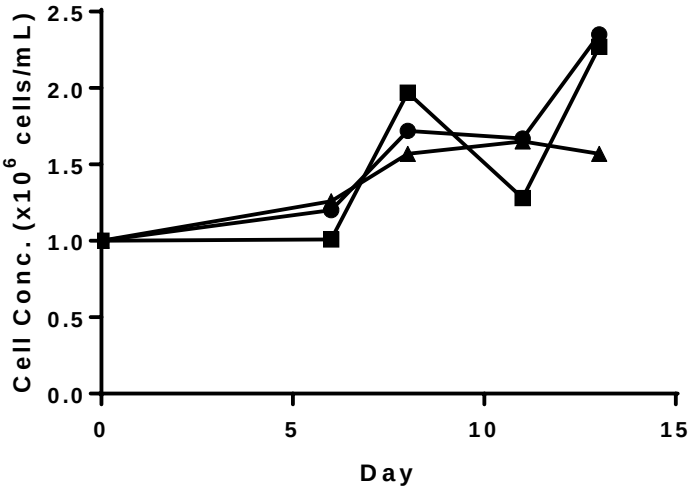

Figure 10: Cell Concentration of NK Cells with IL-15, and without Feeder Cells Each symbol represents different donors.

4.2 FEEDER CELLS WITH MEMBRANE BOUND CYTOKINES SUPPORTS RAPID EXPANSION

NK cells cultured without any feeder cells resulted only a few folds expansion over 14 days as described in 4.1. Next, the NK cells, at 0.2 x 10^6 cell/mL initially, were

co-cultured with four different types of K562 cells that had been irradiated at 10,000 cGy as artificial Antigen Presenting Cells (aAPCs). The four types of K562 cells were: Native K562, K562 with membrane bound IL-15 (K562.mbIL15), membrane bound IL-10 (K562.mbIL10), and membrane bound IL-21 (K562.mbIL21). The growth curves are shown in Figure 11. The numbers of fold expansion are shown in Figure 12.

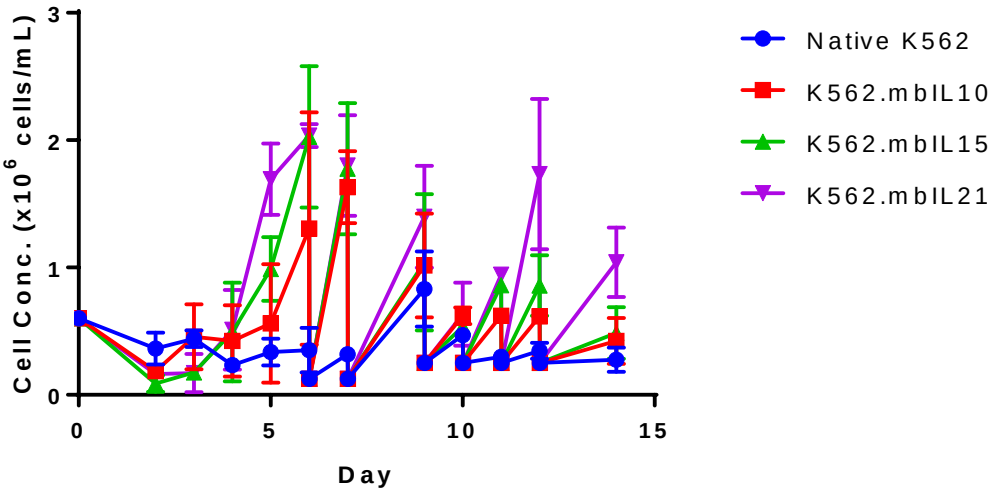

Figure 11: Cell Concentration During the K562 aAPC Co-Cultivation

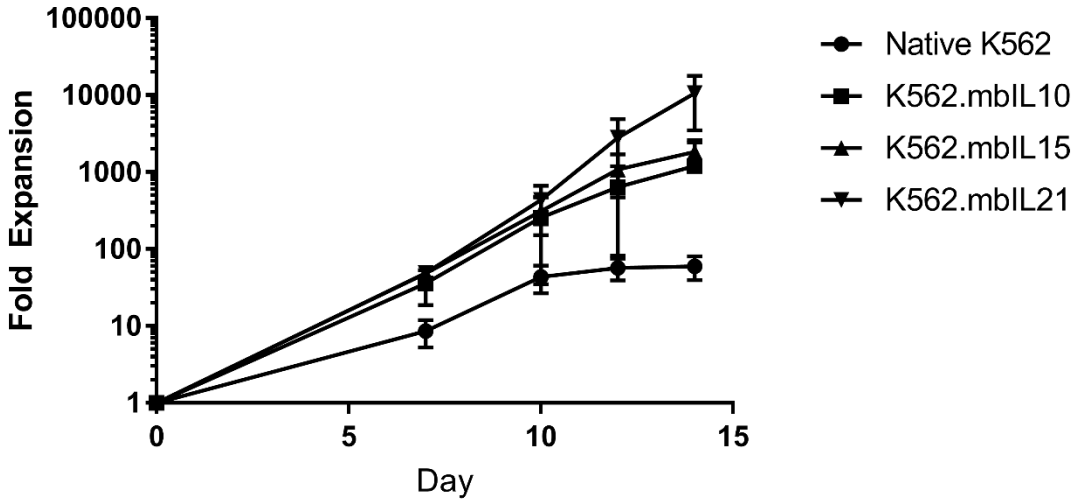

Figure 12: NK Cell Fold Expansion during the Co-Cultivation with K562 aAPCs

It was questionable how long can K562.mbIL21 promote such a rapid expansion. Beyond 14 days cultivation, one donor was selected, and the cultivation was continued beyond 14 days. After 33 days, the growth rate started slowing down, and was not able to reach previously achieved growth rate after re-stimulation. On Day 35, the number of fold expansion reached 100 billion-fold.

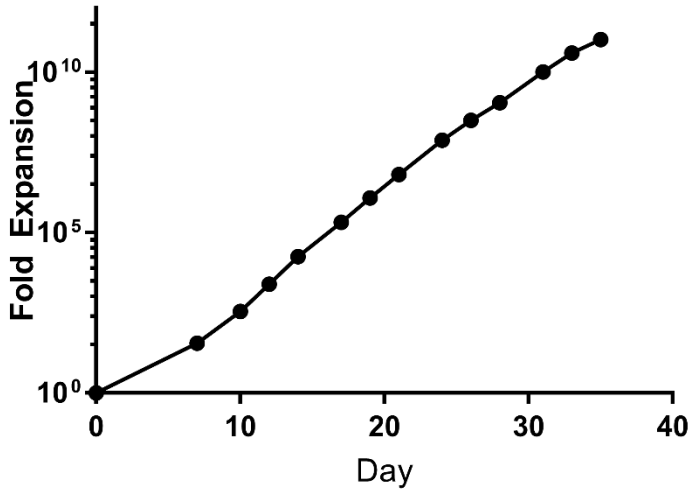

Figure 13: NK Cell Expansion for Extended Period

4.3 CO-CULTURE WITH FEEDER CELLS REGULATE SURFACE RECEPTORS

There are a number of receptors expressed on the surface of NK cell to determine the functionality of the cell. Among them, Killer Ig-like Receptors (KIRs) are inhibitory receptors that balance the activation signals from activating receptors, and also related to acquisition of the core function of NK cell (Cichocki et al; 2010). KIRs are composed of KIR2DL1 (CD158), KIR3DL1 (CD158j), KIR2DL2 (CD158b). Three types of antibodies that can capture all three different KIR were used to capture the level of KIR expression on NK cells. Over 14 days of culture period, the level of KIR expression were upregulated regardless of the type of molecules expressed on the surface of K562 aAPC as well as Native K562.

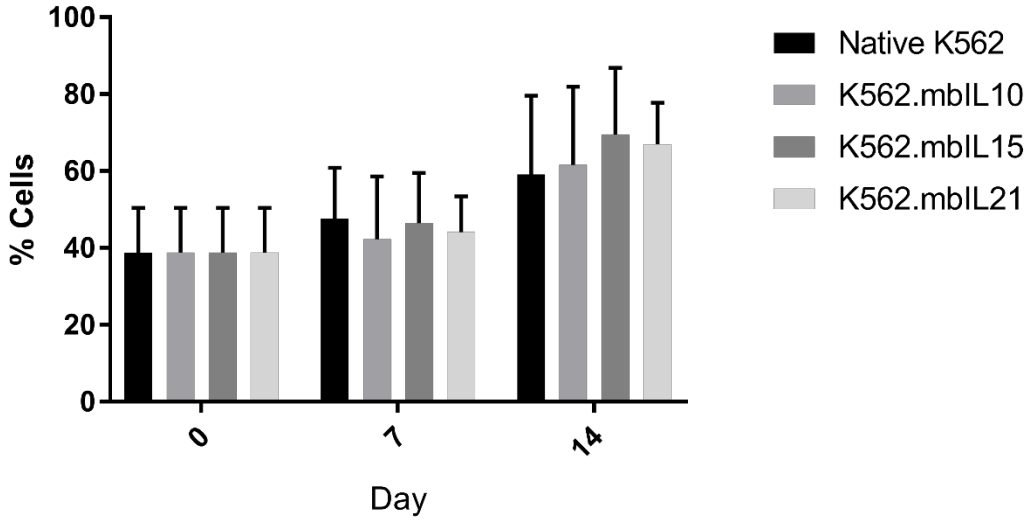

Figure 14: 3KIRs Expression on NK cells expanded on K562 aAPCs

NKp30 is one of the activating receptors that recognize specific ligands on the target cells. While the expression of NKp30 was less than 20% of all NK cell population on Day 0, more than half of NK cell populations activated with all types of K562 aAPCs and Native K562 expressed NKp30.

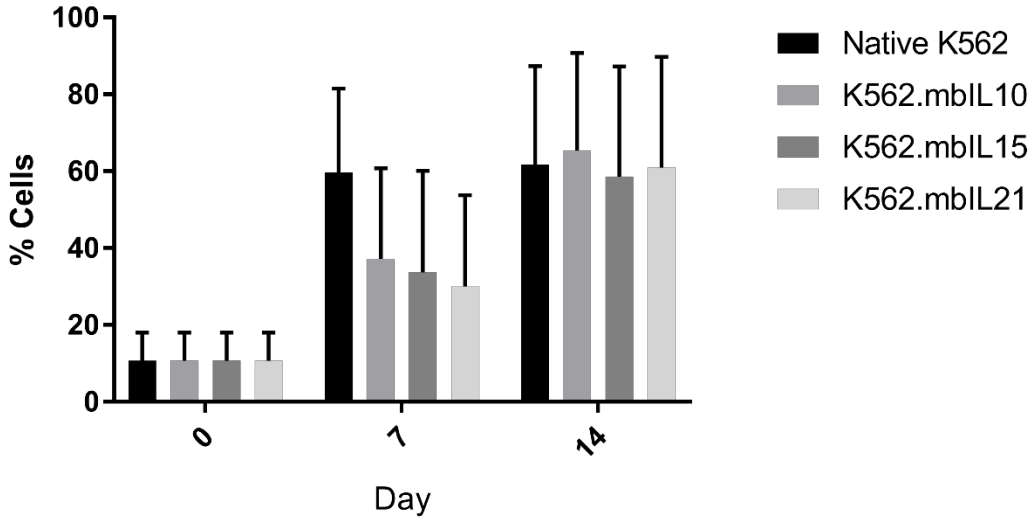

Figure 15: NKp30 Expression on NK cells expanded on K562 aAPCs

CD16 is another type of activating receptors that is also known as Fc receptor. It allows the cell to recognize the target cells coated with antibody, and thus enables antibody-dependent cell cytotoxicity (ADCC, Vivier et al; 2004). While all types of K562 were able to main high level of CD16 expression, K562 aAPCs were able to support even higher level of CD16 expression on NK cells after co-culture.

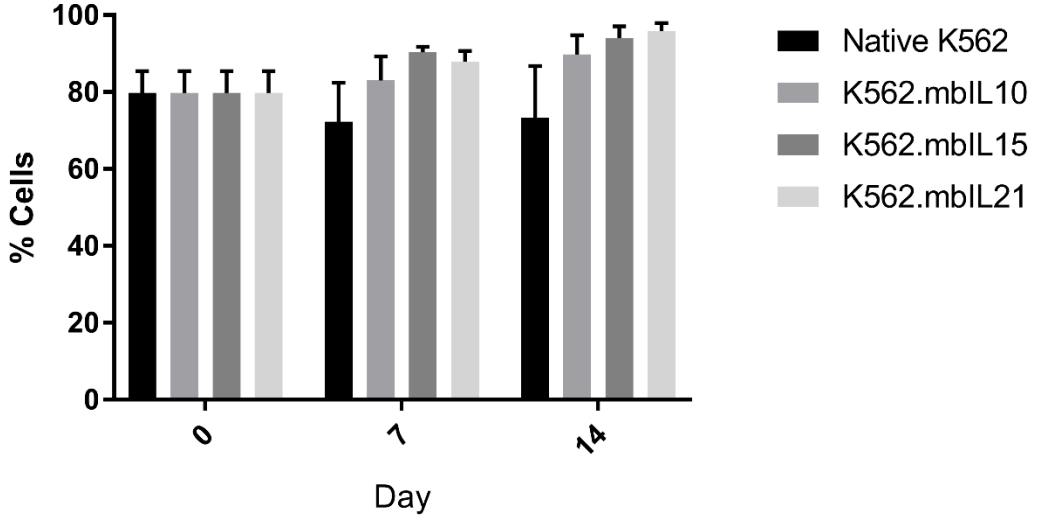

Figure 16: CD16 Expression on NK cells expanded on K562 aAPCs

Even though NK cells rely on the expression of MHC Class I to identify the target, NKG2D is expressed on the surface of NK cells as a homodimer, and recognize non-classical MHC molecules such as MICA and MICB, and also non-MHC molecules such as ULBP1-6. Those non-classical and non-MHC molecules are expressed in response to either viral infection or tumor formation on the cells. (Foley et al; 2014). The expression of NKG2D was close to none on Day 0, but showed highest expression on Day 7. Among four different types of K562, the one bearing cytokine IL-21 was able to upregulate NKG2D the most compared to other types of K562.

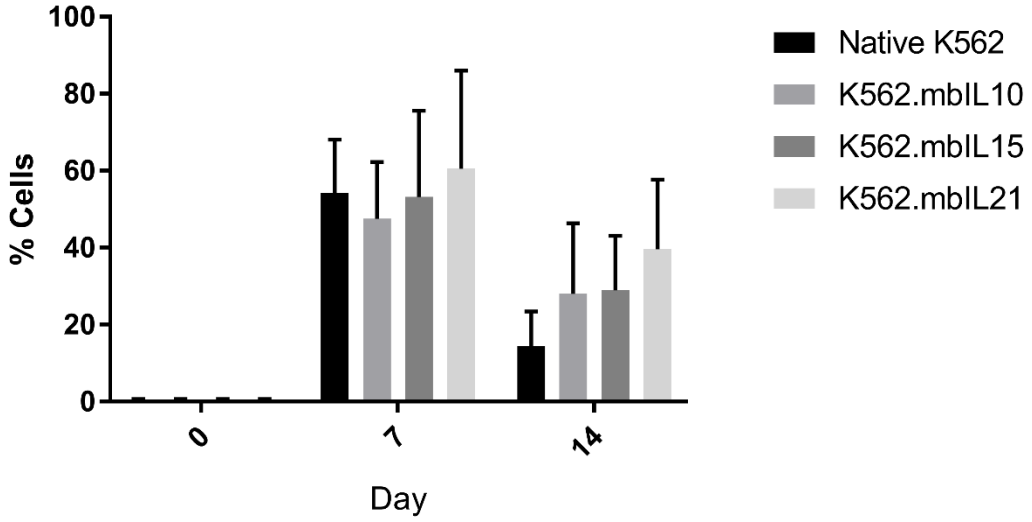

Figure 17: NKG2D Expression on NK cells expanded on K562 aAPCs

LFA-1 (CD11a) is an adhesion molecule that when NK cells encounter the target cells, adhesion through β_2 integrin LFA-1 happens so that a process of lysis can begin. Recent research has discovered that LFA-1 is not only responsible for adhesion with the target, but also transmit activation signals during the early stage of lysis (Barber et al; 2004). Cultivation with K562 upregulated the level of LFA-1 expression on NK cells. By Day 14, NK cells co-cultivated with K562.mbIL21 showed higher expression of LFA-1 compared to others.

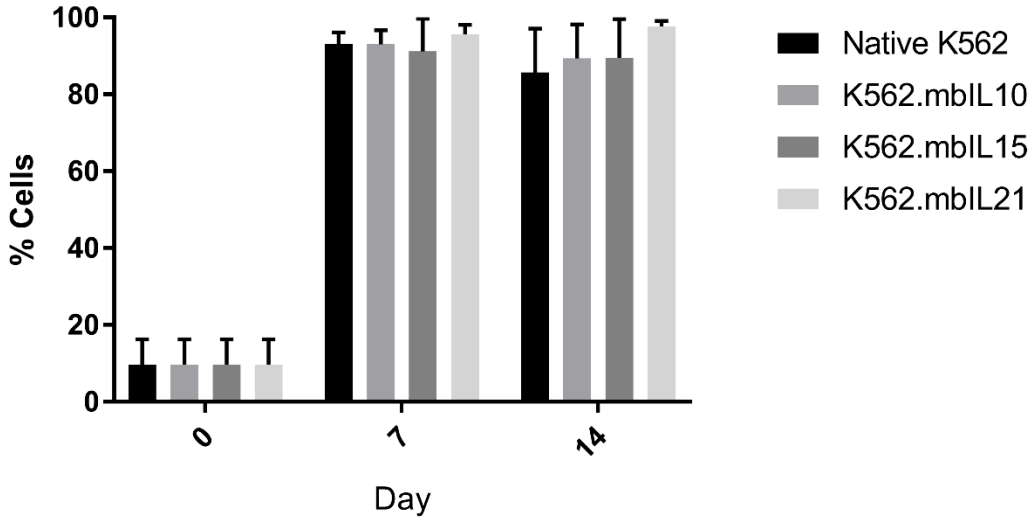

Figure 18: LFA-1 Expression on NK cells expanded on K562 aAPCs

NKG2C (CD94) is an activating receptor that belongs to C-type lectin superfamily that binds to HLA-E (Lanier et al; 1998) It is also reported that NKG2C is expressed on expanding NK cell subsets caused by human cytomegalovirus (HCMV) or other viruses (Schlums and Cichocki et al; 2015). It was rare to find a donor with high level of NKG2C expression on Day 0. Most donors in this experiment showed rather low levels of NKG2C initially. After co-cultivation, most NK cells showed higher levels of NKG2C compared to Day 0.

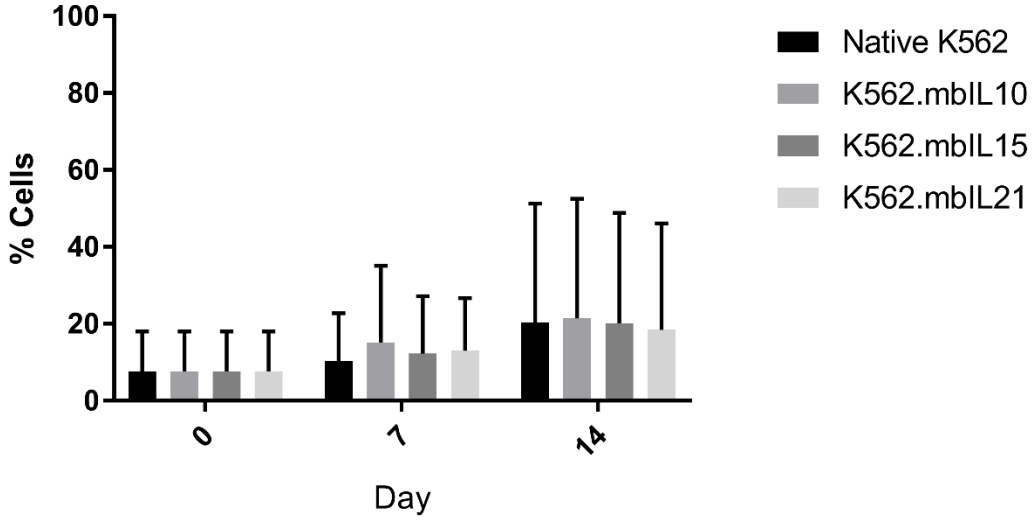

Figure 19: NKG2C Expression on NK cells expanded on K562 aAPCs

Not much is known about CD96. It is a member of Ig family that shares the ligand CD155 with CD226 and TIGIT. CD155 is the main ligand for CD96 (Chan et al; 2014). NK cells cultured with K562.mbIL21 showed higher expression of CD96 in general, but the expression faded away after Day 7.

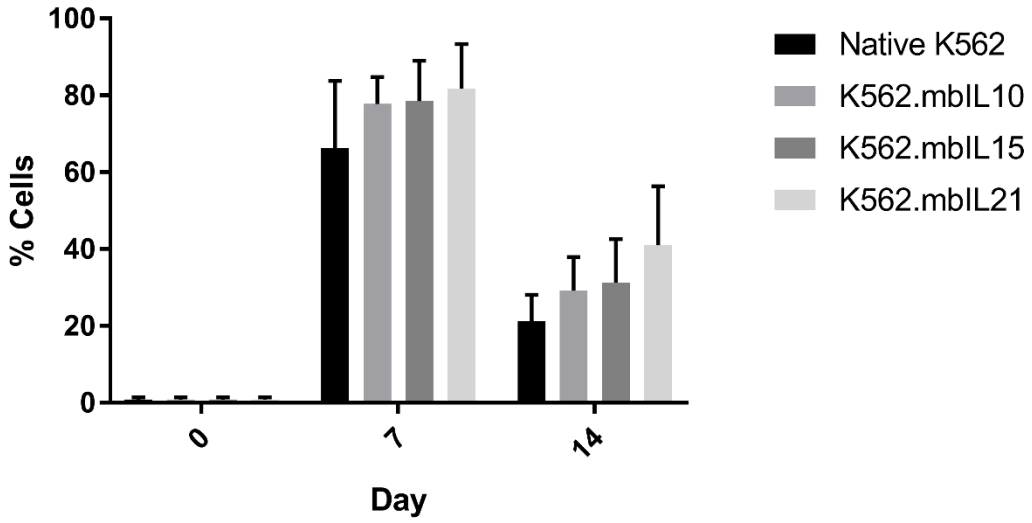

Figure 20: CD96 Expression on NK cells expanded on K562 aAPCs

CD2 is another type of adhesion molecule on the surface of NK cells. Day 0 NK cells showed moderate level of CD2 expression, and the level of expression was upregulated during the co-cultivation. Both Day 7 and 14 NK cells were able to retain high level of CD2 expression.

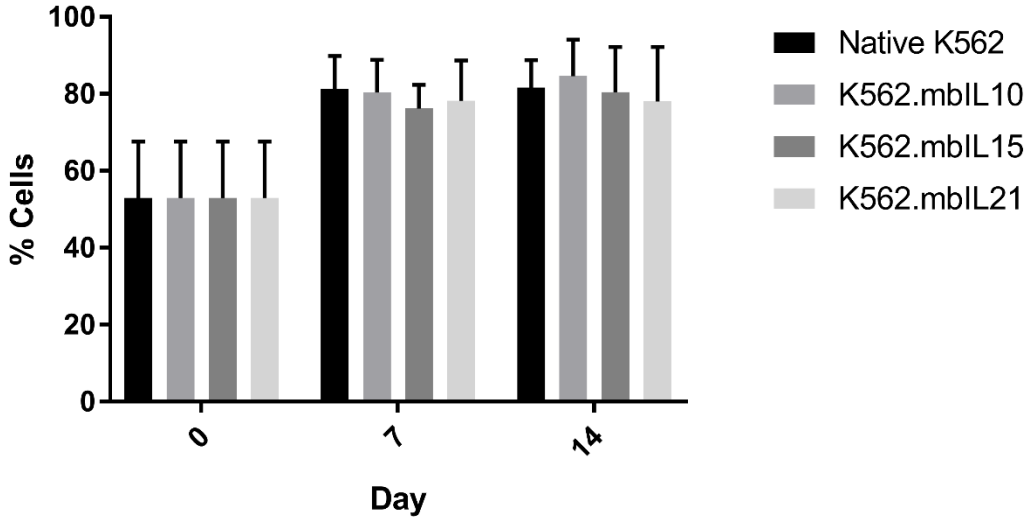

Figure 21: CD2 Expression on NK cells expanded on K562 aAPCs

NKG2A, also known as CD159a, is an inhibitory receptor that forms a heterodimer with CD94. The heterodimer binds to HLA-E, which is a type of non-classical MHC class I. NK cells showed relatively low level of NKG2A expression on Day 0. After the co-culture, NKG2A was upregulated on Day 7. By Day 14, it showed higher level of NKG2A, but slightly lower compared to Day 7.

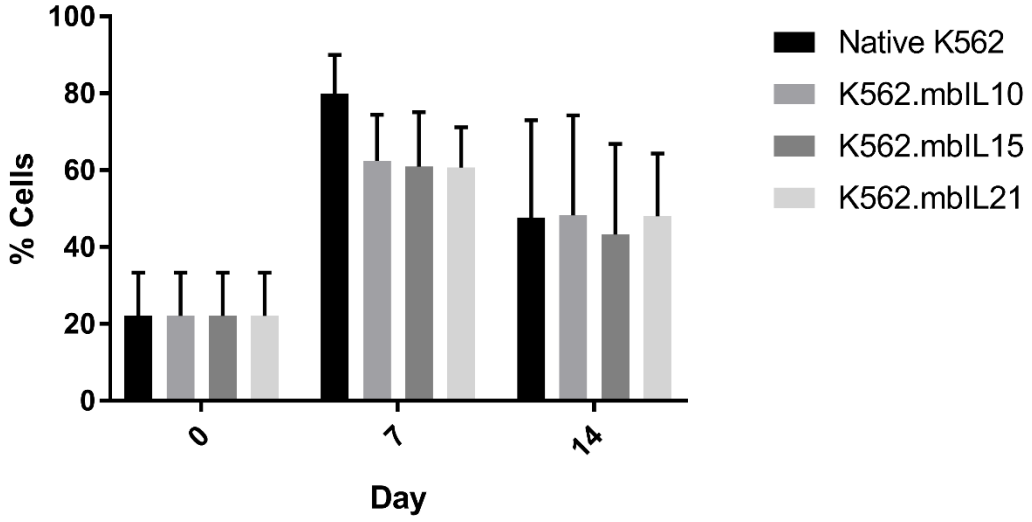

Figure 22: NKG2A Expression on NK cells expanded on K562 aAPCs

CD81 was identified as a protein that inhibits lymphocyte proliferation. In addition, it was identified to be a marker of hepatitis C virus (HCV) infection of hepatocytes. Once HCV binds to CD81 on NK cells, it will inhibit killing and cytokine production by NK cells (Crotta et al; 2002). Initially shown at a low level of expression of CD81, more than half of the population expressed CD81 on Day 7, and the expression slightly diminished on Day 14.

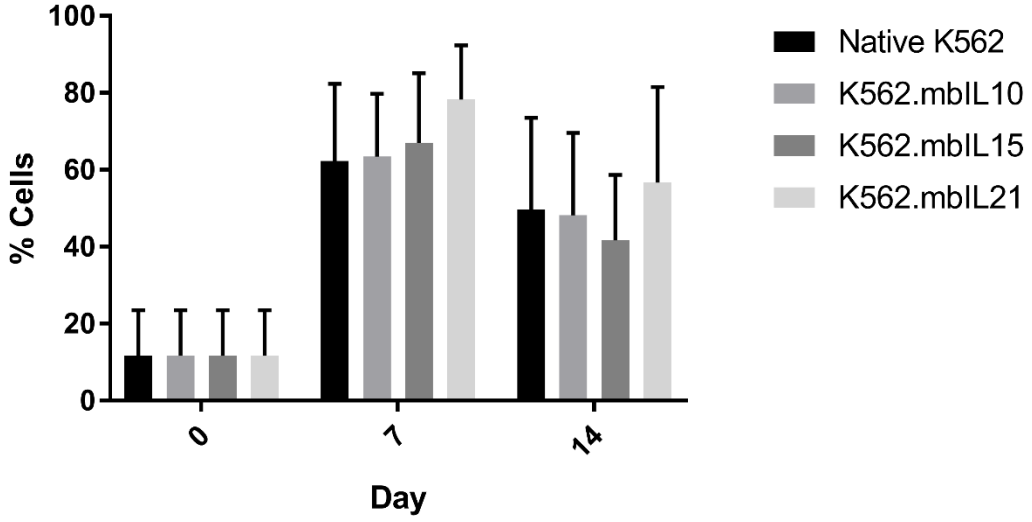

Figure 23: CD81 Expression on NK cells expanded on K562 aAPCs

CD45 is a big family of multiple isoforms that are coming from a single gene. CD45RA is known to be expressed on naïve T cells and resting NK cells. As cells become activated, CD45RA losses its expression, and another isoform, named CD45RO, is expressed. CD45RO is expressed on activated and memory T cell and activated NK cells. As shown in the figure, CD45RA is expressed at a high level on Day 0, and losses its expression over the course of co-cultivation. CD45RO is almost not captured on Day 0, but becomes highly expressed on Day 7 and 14.

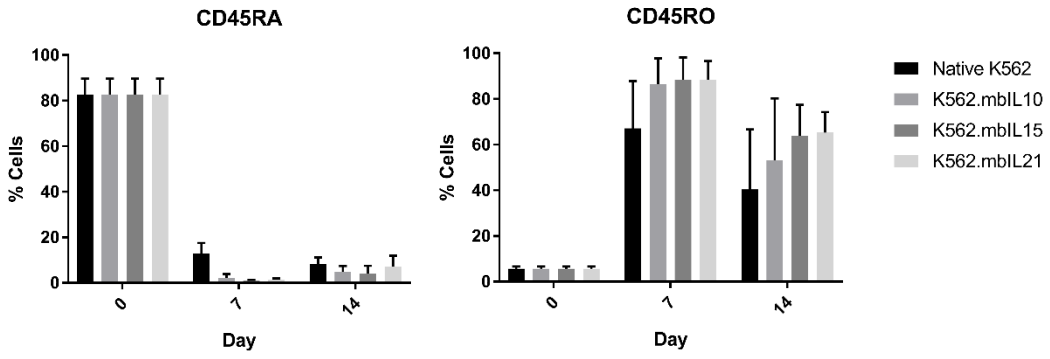

Figure 24: CD45RA, CD45RO Expression on NK cells expanded on K562 aAPCs

CD44 is responsible for lympho-hemopoiesis, adhesion to high endothelial venules or the extracellular matrix, and T cell activation. Ligation of CD44 has shown enhanced cytotoxic activity of NK cells (Galandrini et al; 1994). Over the course of co-cultivation, CD44 expression stayed at a relatively low level. NK cells co-cultivated with Native K562 showed higher level of CD44 expression on Day 7, but it faded away by Day 14.

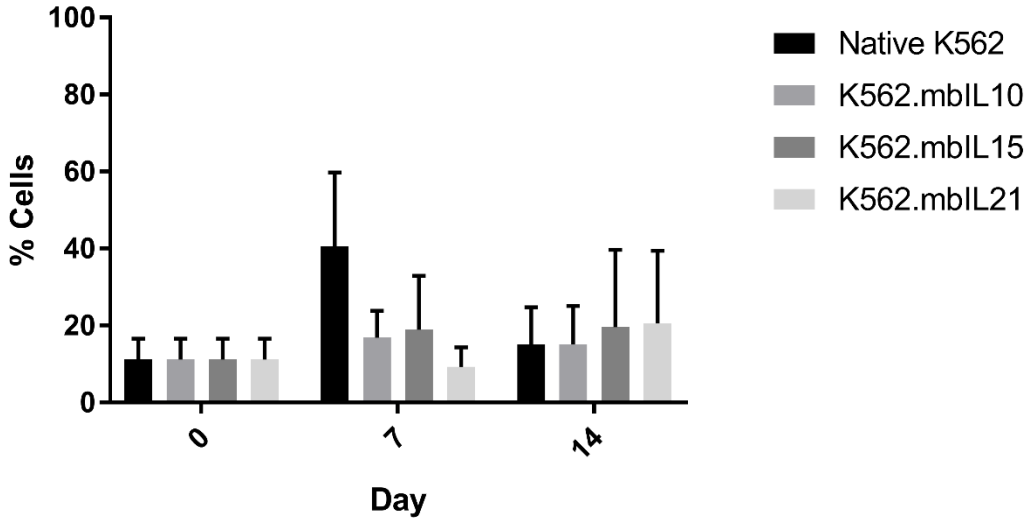

Figure 25: CD44 Expression on NK cells expanded on K562 aAPCs

4.4 MULTI-DIMENSIONAL FLOW CYTOMETRY ANALYSIS BY SPADE

Flow cytometry data from NK cells cultivated from five donors with IL-21 membrane bound K562 was concatenated, and tested to see the changes of proportion over time for certain phenotypes.

There were three panels tested to accommodate multiple markers. The first panel was clustered with 9 markers, 3KIRs, NKp30, CD319, CD62L, 2B4, CD16, NKG2D, CD57, and CD117. Among the 9 markers, only 3KIRs, NKp30, CD16, and NKG2D were annotated since they showed clear separation for annotation. There were four different phenotypes defined.

Group A represents $3KIRs^{-}NKp30^{-}CD16^{+}NKG2D^{-}$. Group B represents $3KIRs^{+}NKp30^{-}CD16^{+}NKG2D^{+}$. Group C represents $3KIRs^{-}NKp30^{+}CD16^{+}NKG2D^{+}$. Group D represents $3KIRs^{+}NKp30^{+}CD16^{+}NKG2D^{+}$.

Group A, which was dominating population on Day 0, showed its dominance on Day 0, but was differentiated into activated forms on Day 7 and 14. Group B and C were intermediates during the activation, and were well captured on Day 7. Group D showed highest proportion on Day 14.

By using this SPADE analysis, SPADE figures were generated (Figure 26, Figure 27, Figure 28) to visualize the cell differentiation over time, and also the proportion of each donor was plotted in a bar chart to show the difference between donors (Figure 29, Figure 30, Figure 31).

Panel 2 consisted of 8 makers clustered, LFA-1, NKG2C, CD96, ILT2, TIGIT, TIM-3, CD2, and CD57, and only LFA-1, CD96, and CD2 were annotated.

Group A represents LFA-1^{-} CD96^{-}CD2^{+}. Group B represents LFA-1^{+} CD96^{+}CD2^{+}. Group C represents LFA-1^{+} CD96^{-}CD2^{+}. Group A was the dominating phenotype on Day 0, Group B was on Day 7, and both B and C dominated on Day 14. In this panel, Group B could be considered the idealistic phenotype, but it lost some of its expression of CD96 on Day 14, thereby it became the phenotype Group C, which lacks CD96 expression. The reason why CD96 loses its expression after it peaked on Day 7 will require further investigation.

Panel 3 consisted of 8 markers clustered, CD164, NKG2A, CD52, CD81, CD45RO, CD45RA, CD44, and CD57. Four of them, NKG2A, CD81, CD45RO, CD45RA, were annotated. Group A represents NKG2A^{-}CD81^{-}CD45RO^{-}CD45RA^{+}. Group B represents NKG2A^{+}CD81^{+}CD45RO^{+}CD45RA^{-}. Group C represents NKG2A^{-}CD81^{+}CD45RO^{+}CD45RA^{-}.

In this panel, it is good to have NKG2A and CD81 expressed, but CD45RA is expressed on naïve T cell or resting NK cells, and CD45RO is expressed on effector T cell or activated NK cells. Therefore, the idealistic phenotype in this panel should have NKG2A, CD81, and CD45RO expressed, which is presented as Group B.

Group A dominated on Day 0, whereas Group B and C dominated on Day 7 and 14. It is questionable why Group B is not maintained at a high proportion during the co-cultivation, which requires further investigation.

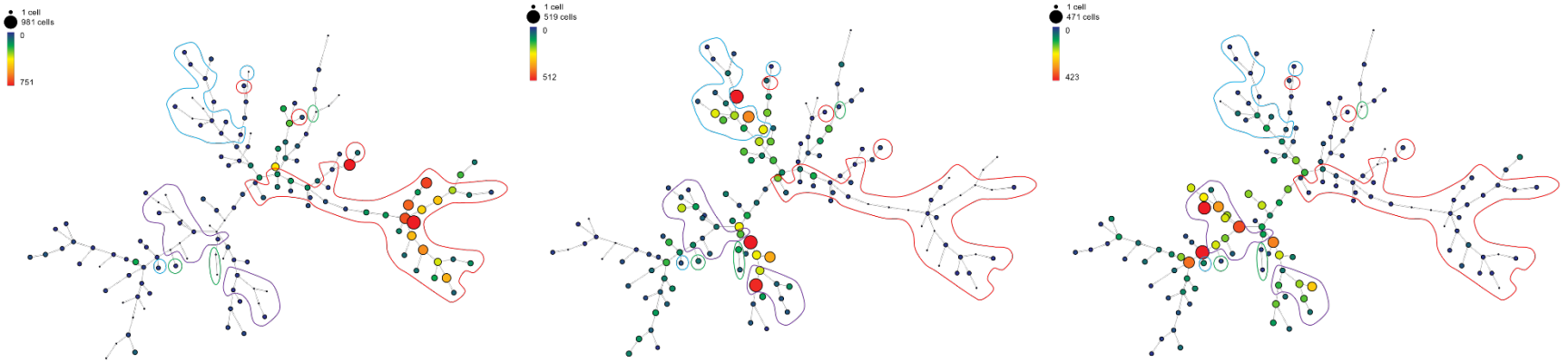

Group	A	B	C	D
%	70.08	0.01	0.39	0.19

Group	A	B	C	D
%	6.53	5.80	16.41	19.36

Group	A	B	C	D
%	4.19	1.84	5.53	31.95

Figure 26: Day 0, 7, and 14 (Left to Right) SPADE Analysis of donor SLR833. Panel 1.

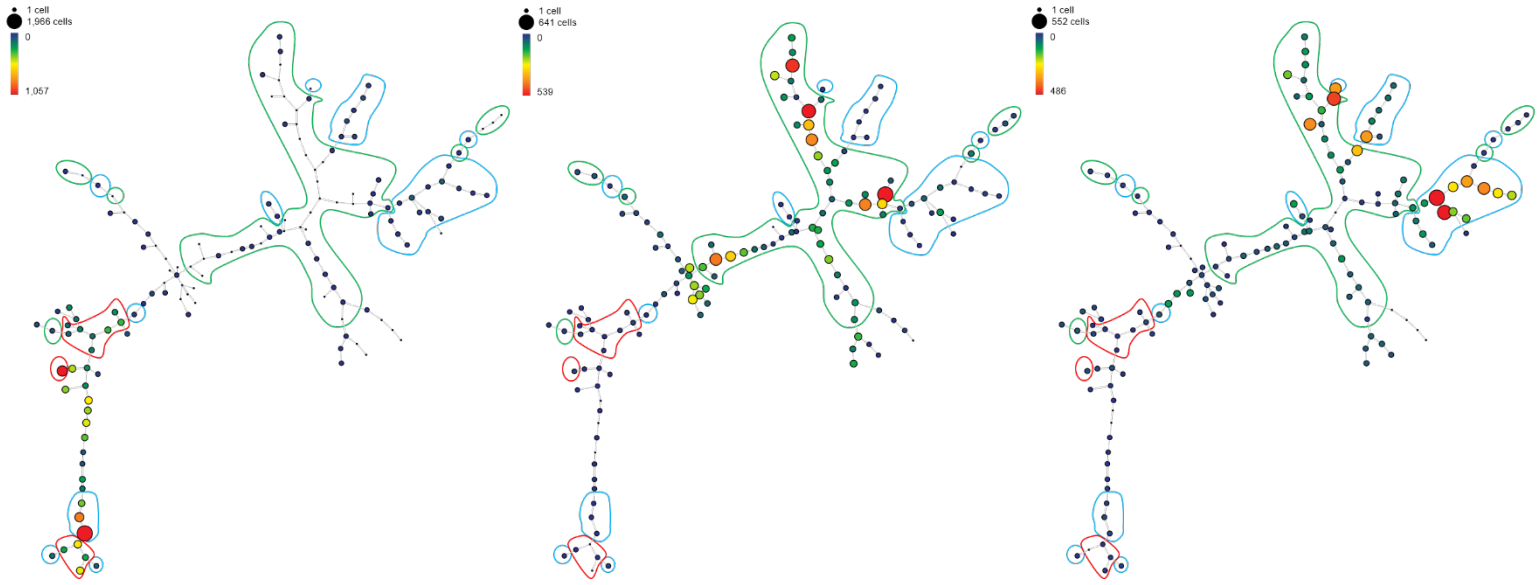

Group	A	B	C
%	31.78	1.50	32.10

Group	A	B	C
%	0.85	74.43	4.39

Group	A	B	C
%	1.43	39.62	48.28

Figure 27: Day 0, 7, and 14 (Left to Right) SPADE Analysis of donor SLR833. Panel 2.

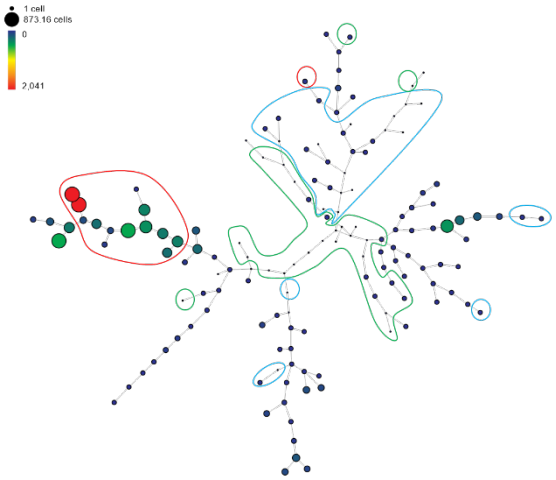

Group	A	B	C
%	62.02	0.21	0.57

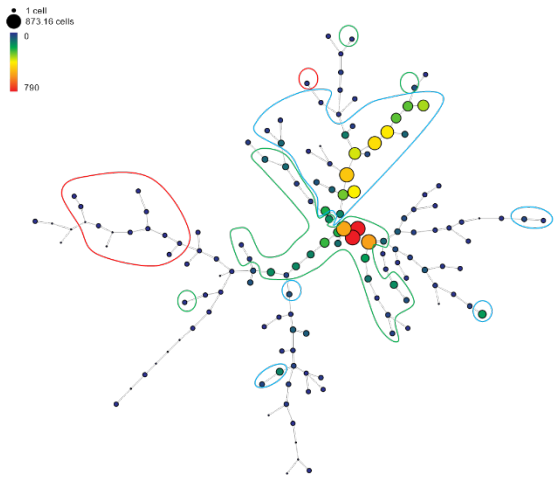

Group	A	B	C
%	0.29	46.43	44.30

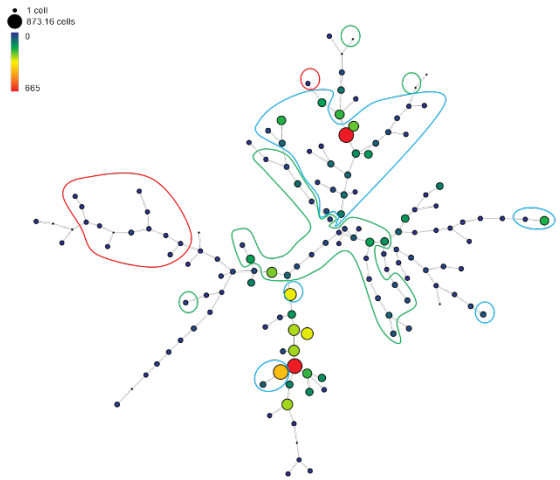

Group	A	B	C
%	0.83	16.24	38.37

Figure 28: Day 0, 7, and 14 (Left to Right) SPADE Analysis of donor SLR833. Panel 3.

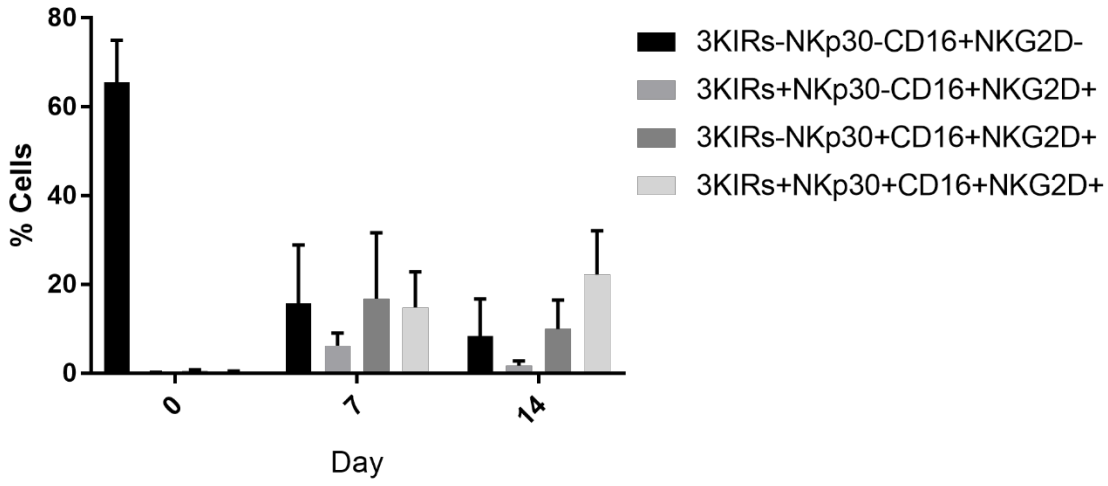

Figure 29: Phenotype group proportion changes over time for Panel 1.

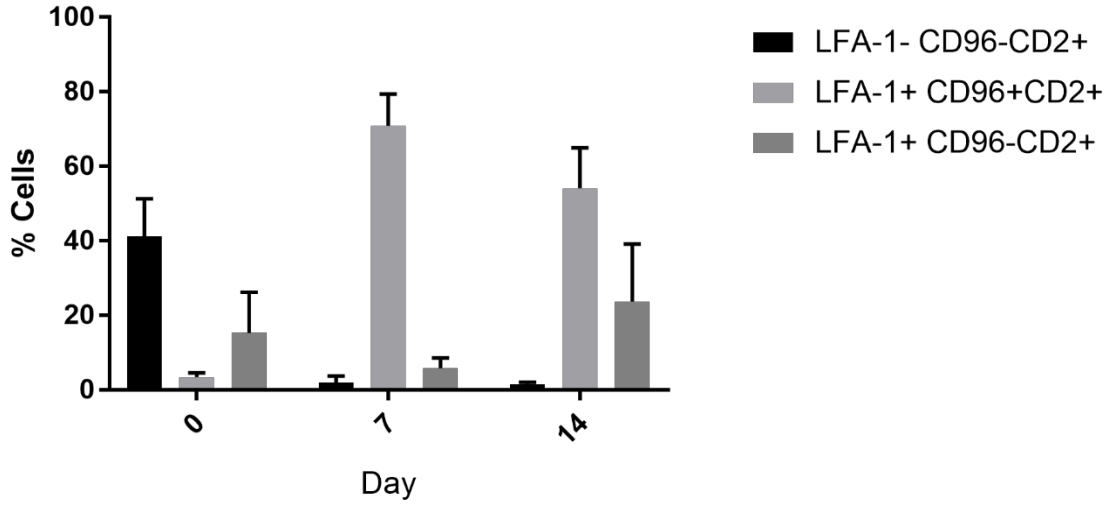

Figure 30: Phenotype group proportion changes over time for Panel 2.

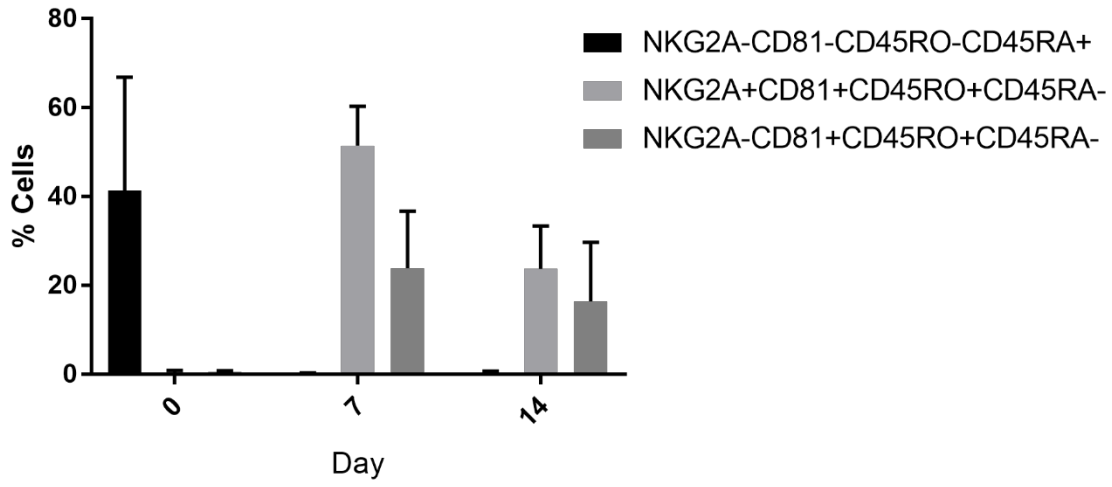

Figure 31: Phenotype group proportion changes over time for Panel 3.

4.5 GLUCOSE AND OXYGEN CONSUMPTION PROFILE

Glucose measurement was plotted in Figure 33 showing cumulative consumption of glucose. The consumption at the beginning of the culture was higher than usual due to the K562 cells consumed glucose until they were lysed by NK cells. At the beginning, the ratio between NK cell and K562 cells was approximately 1:10, whereas re-stimulation on Day 7 required only 1:1 ratio, which did not give significant impact on glucose consumption. While the number of cell reached 10 billion compared to the initial cell population of approximately 1.6 million cells, cells consumed total of about 70 mmol of glucose over the 14-day cultivation.

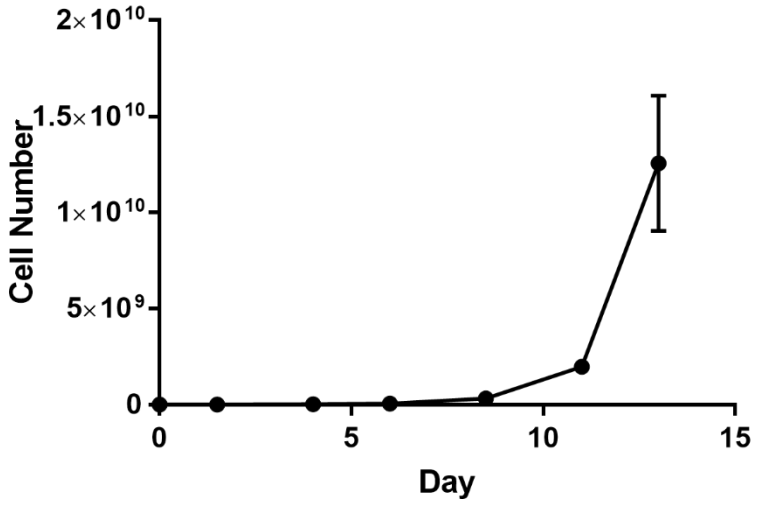

Figure 32: Cumulative cell number during glucose measurement

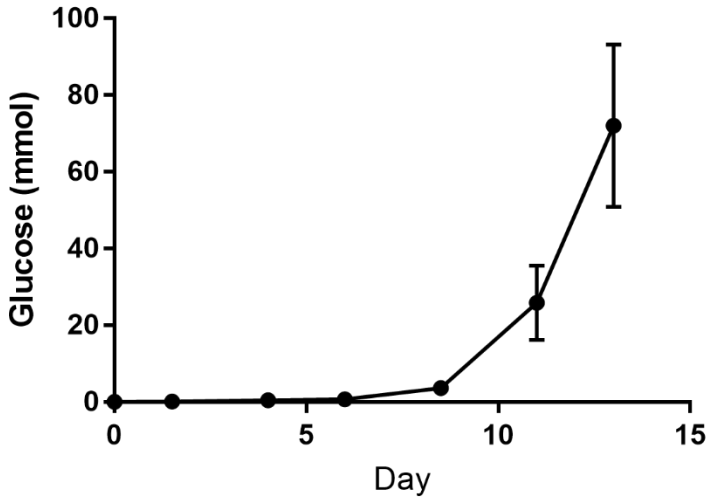

Figure 33: Cumulative glucose measurement

4.6 COLLECTION OF KINETIC PARAMETERS OF NK AND K562 CULTURES

4.6.1 NK Cells

Cell Size

NK cells isolated from one donors and depleted with CD3 and CD19 cells as described in Materials and Methods were inoculated in a T-75 flask at 0.4 x 10^6 cells/mL. A 1-mL sample was collected on Day 3 of the culture, and measured the cell size distribution with Vi-Cell XR Analyzer. Mean diameter of NK cells was 10.81 x 10^{-6} m, and standard deviation of the mean diameter was 3.46 x 10^{-6} m. The distribution diagram was shown in Figure 34.

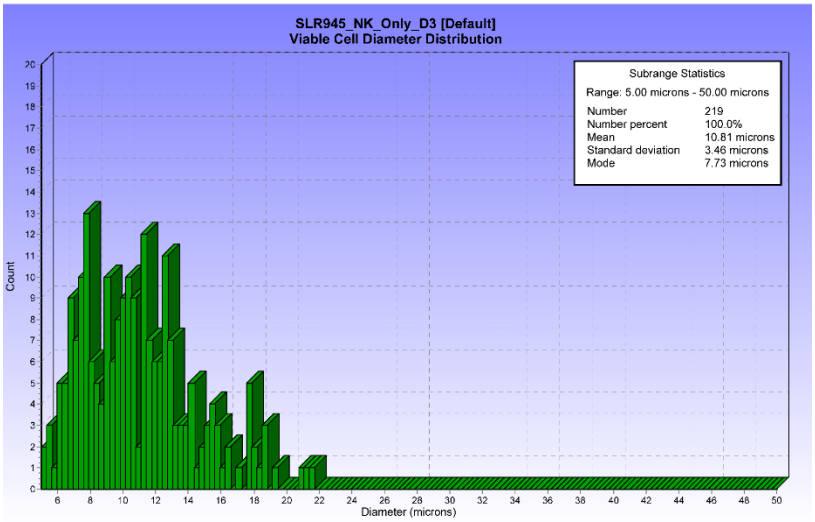

Figure 34: NK Cell Diameter Distribution

Specific Rate Amino Acids

NK cells were isolated from PBMCs using magnetic bead depletion of CD3 and CD19 cells. NK Cells were placed in a T-75 flask at a concentration of 0.2 x 10^6 cells/mL. Initially the actual concentration of NK cells from the heterogeneous culture that consists of NK Cell and Monocyte are approximately 1:5; thus, making the approximate cell centration of NK Cells to be 0.04 x 10^6 cells/mL. The NK cells were stimulated by K562.mbIL21 Cells at a ratio of 1:10. Media was changed at Day 3,5,7,10, 12 respectively per descriptions in Materials and Methods. Samples were collected during the media change, and were analyzed by HPLC.

Concentration of amino acids throughout the cultivation was shown in Figure 35, Figure 36, Figure 37, Figure 38.

Specific rate of amino acids consumption or production was shown in Figure 39, Figure 40, Figure 41, Figure 42.

Cumulative rate of amino acids consumption or production was shown in Figure 43, Figure 44, Figure 45.

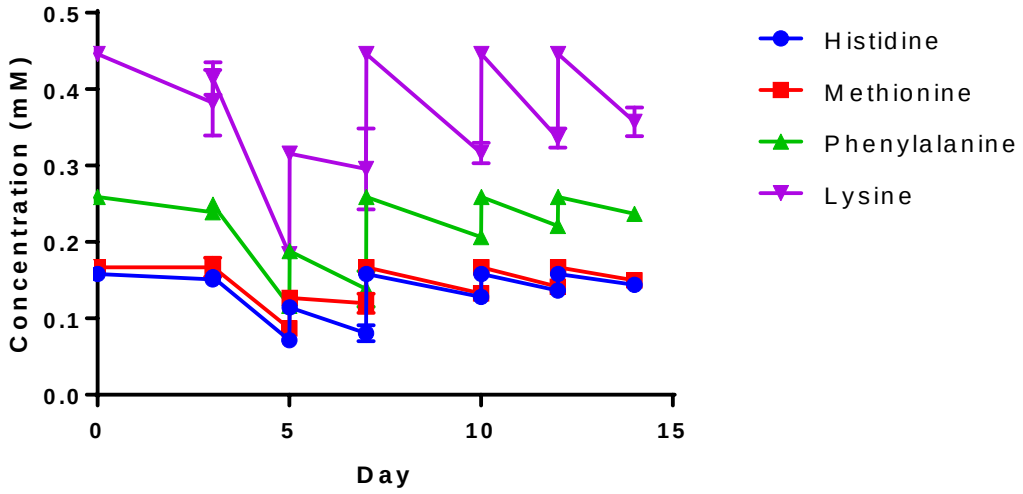

Figure 35: Concentration of Essential Amino Acids Histidine, Methionine, Phenylalanine, Lysine

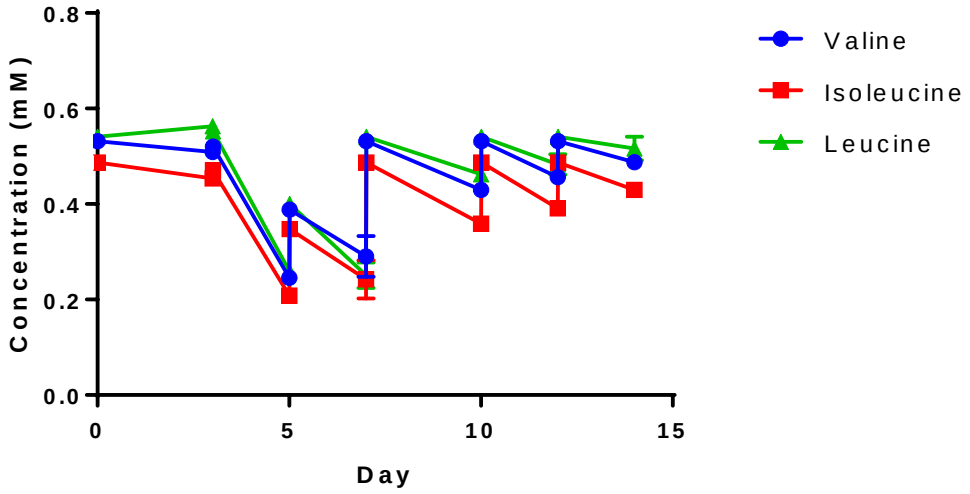

Figure 36: Concentration of Essential Amino Acids Valine, Isoleucine, Leucine

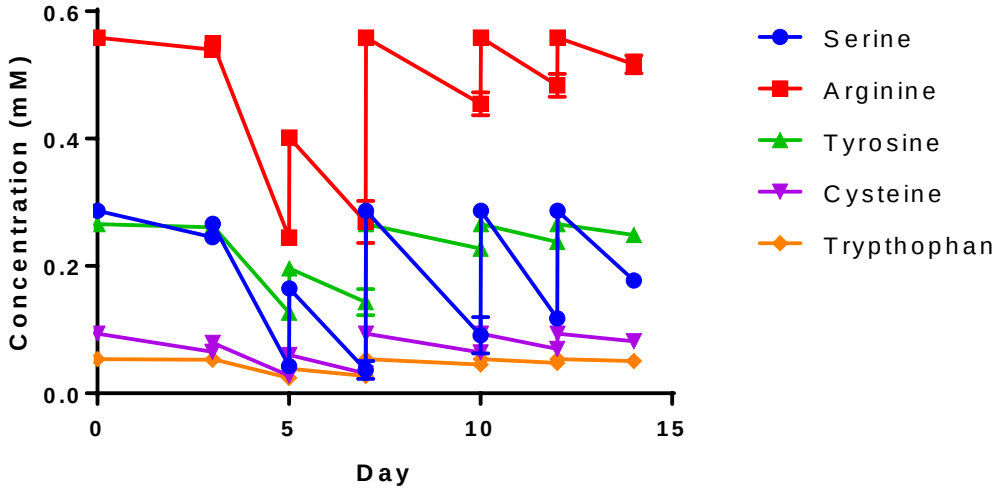

Figure 37: Concentration of Non-Essential Amino Acids Serine, Arginine, Tyrosine, Cysteine, Tryptophan

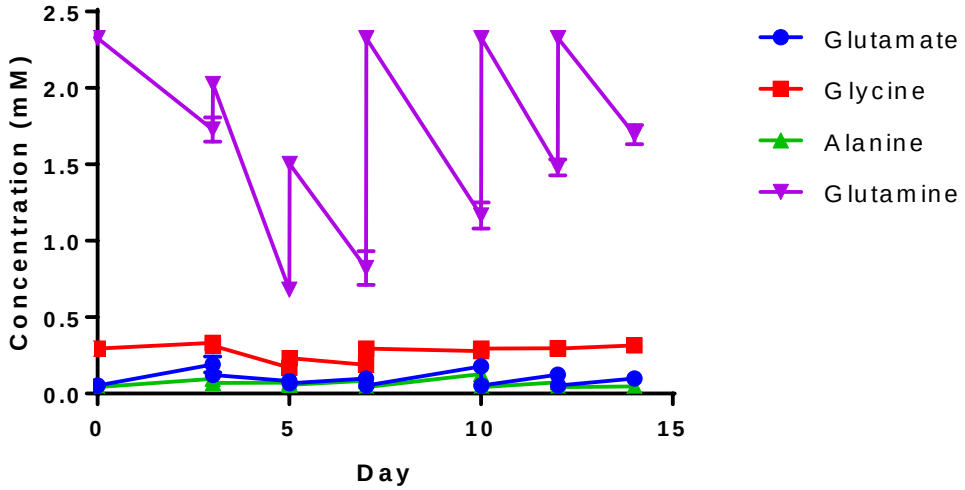

Figure 38: Concentration of Non-Essential Amino Acids Glutamate, Glycine, Alanine, Glutamine

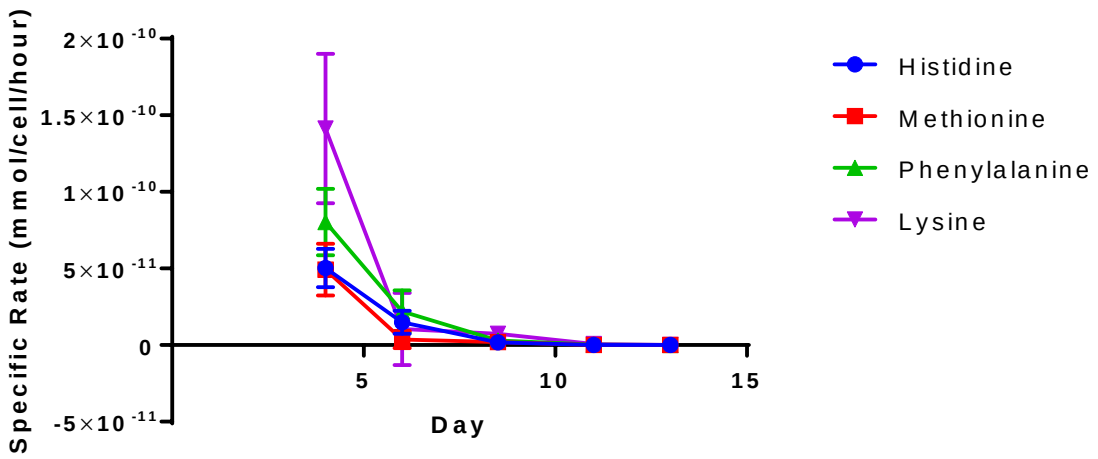

Figure 39: Specific Rate of Essential Amino Acids Histidine, Methionine, Phenylalanine, Lysine

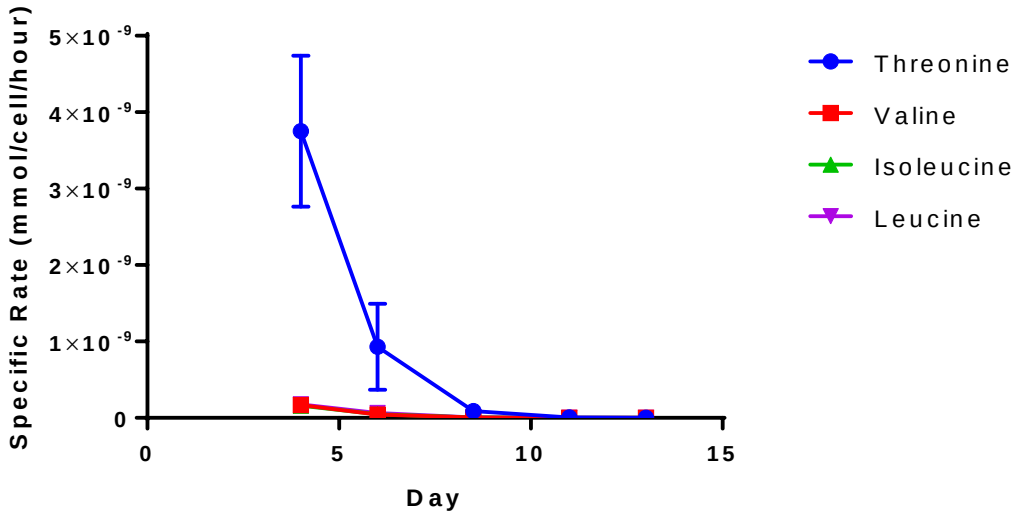

Figure 40: Specific Rate of Essential Amino Acids Threonine, Valine, Isoleucine, Leucine

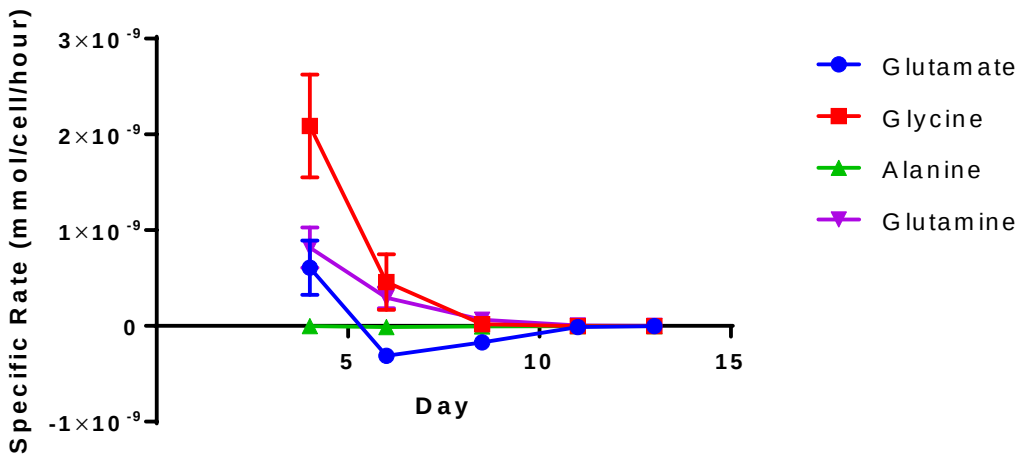

Figure 41: Specific Rate of Non-Essential Amino Acids Glutamate, Glycine, Alanine, Glutamine

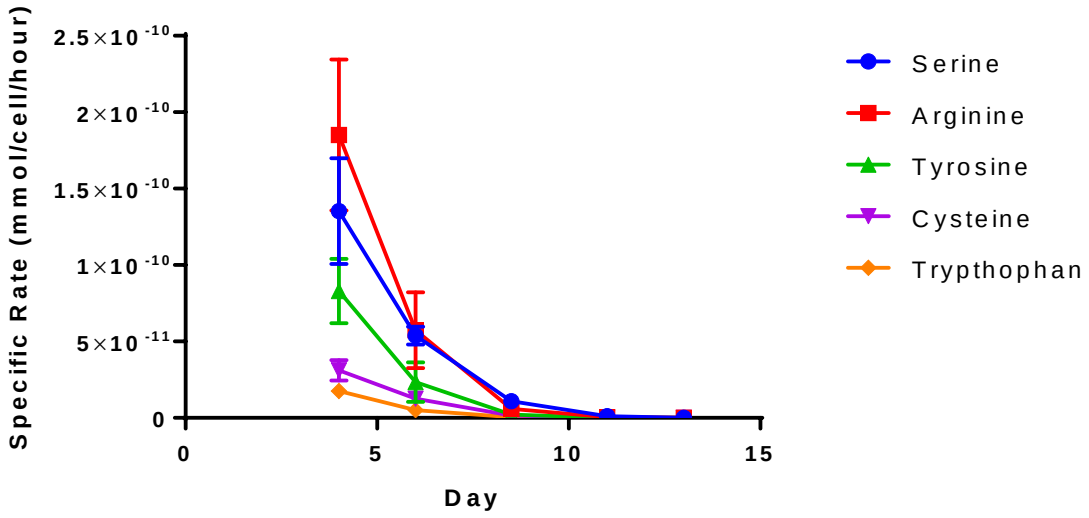

Figure 42: Specific Rate of Non-Essential Amino Acids Serine, Arginine, Tyrosine, Cysteine, Tryptophan

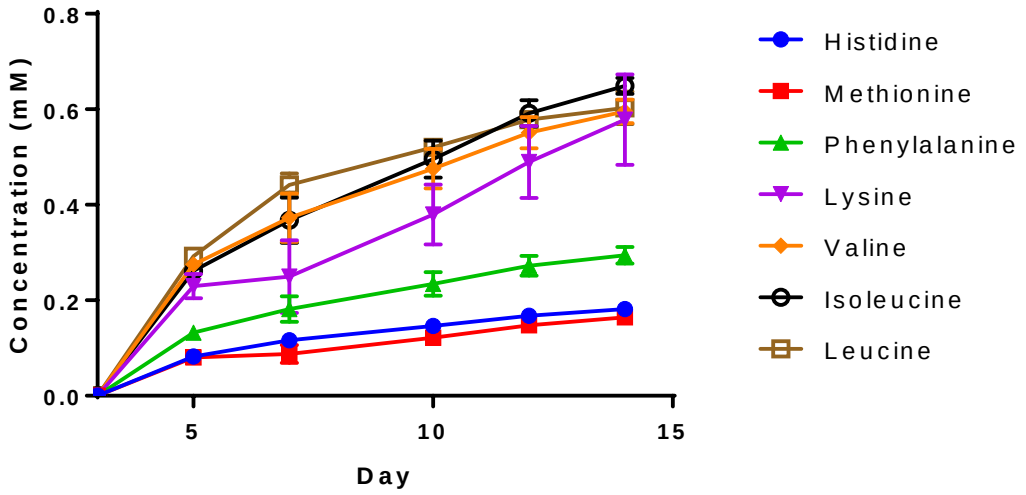

Figure 43: Cumulative Concentration of Essential Amino Acids Histidine, Methionine, Phenylalanine, Lysine, Valine, Isoleucine, Leucine

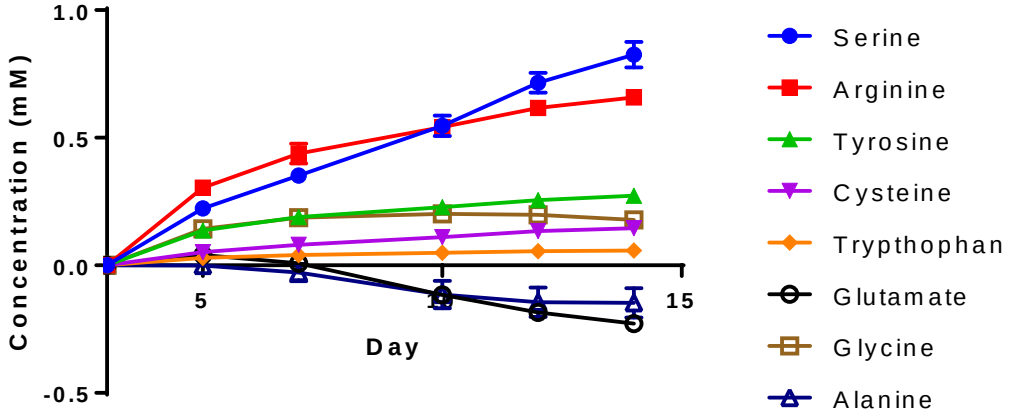

Figure 44: Cumulative Concentration of Non-Essential Amino Acids Serine, Arginine, Tyrosine, Cysteine, Tryptophan, Glutamate, Glycine, Alanine

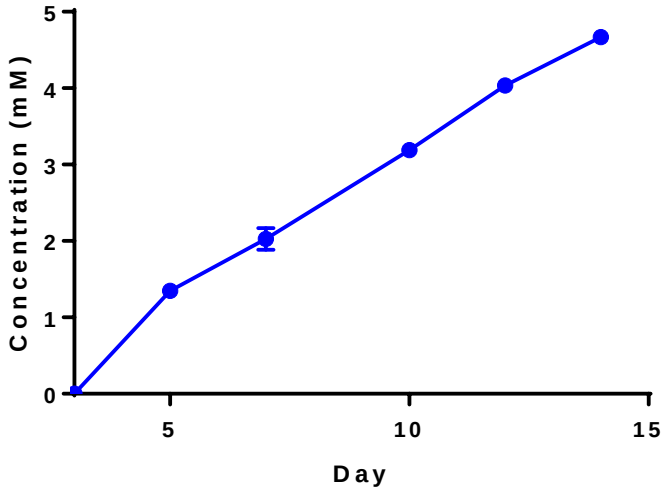

Figure 45: Cumulative Concentration of Non-Essential Amino Acids Glutamine

Specific Consumption Rate of Glucose and Production Rate of Lactate

NK cells were isolated from PBMCs using magnetic beads to enrich CD56 population. Cells were placed in 24 well plate with working volume of 1 mL. The media was supplemented with 50 IU/mL of IL-15. The media was replenished at a full volume on Day 7. Samples were taken on Day 5, 7, 12, 16 respectively, and were analyzed the concentration of glucose and lactate.

Cumulative concentration of glucose consumption and lactate production were shown in Figure 46.

Specific rates of glucose consumption and lactate production were shown in Figure 47.

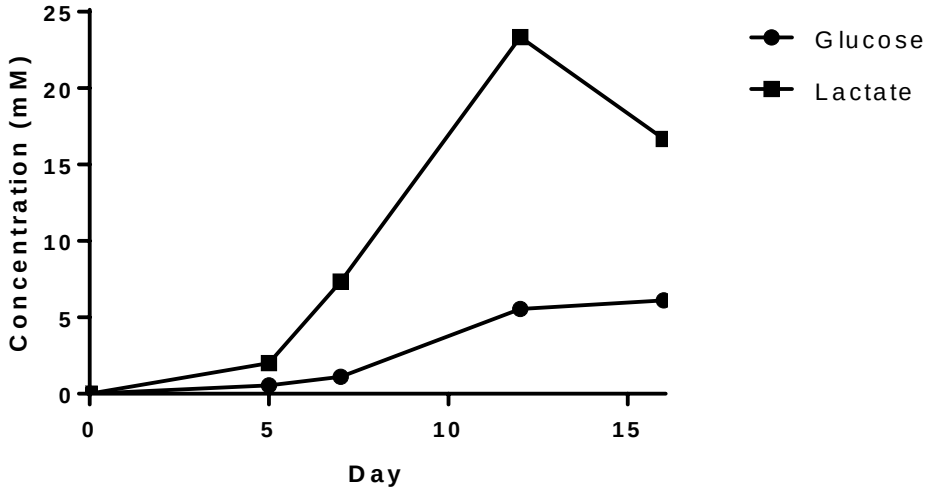

Figure 46: Cumulative Concentration of Glucose Consumption and Lactate Production

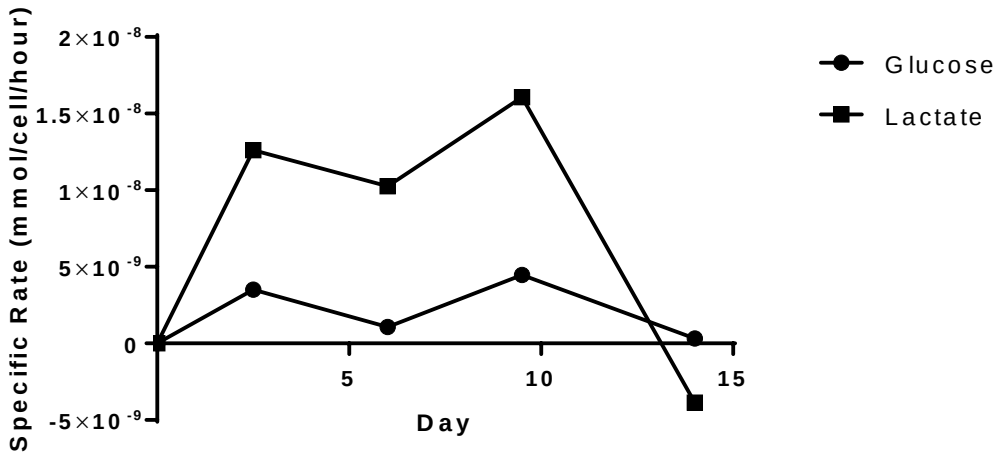

Figure 47: Specific Rate of Glucose Consumption and Lactate Production

Specific Consumption Rate of Oxygen

In order to determine the effect of NK cell activation on the rate of oxygen consumption, pure CD56 populations were isolated from donor's blood using CD56 Enrichment Kit, and started cultivation in T-75 flask using B0 media. Then, the oxygen consumption rate was measured in three different conditions; right after isolation, after three days of cultivation with no feeder cells, after three days of cultivation with K562.mbIL21 (shown in Figure 48). The oxygen consumption rate was the lowest when the cells were isolated from the blood. Compared to the cells cultivated without feeder and with feeder cells, those cultivated with feeder cells showed higher consumption of oxygen that may be caused by activation.

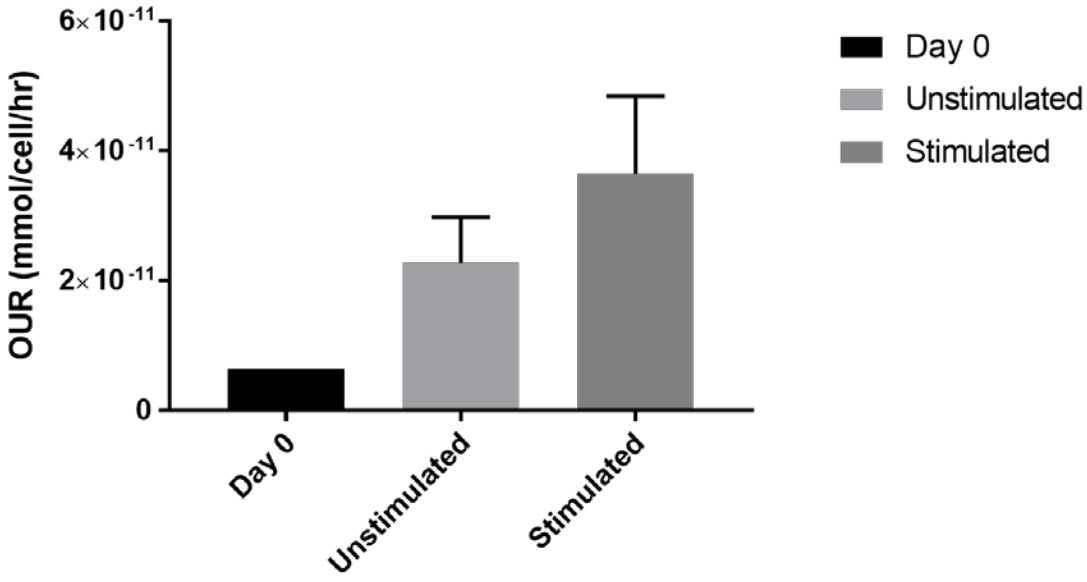

Figure 48: Specific Consumption Rate of Oxygen

4.6.2 K562 Cells

Cell Size

Native K562 cells thawed and were inoculated in a T-75 flask at 0.8 x 10^6 cells/mL. A 1-mL sample was collected on Day 3 of the culture, and measured the cell size distribution with Vi-Cell XR Analyzer. Mean diameter of NK cells was 15.71 x 10^{-6} m, and standard deviation of the mean diameter was 4.09 x 10^{-6} m. The distribution diagram was shown in Figure 49.

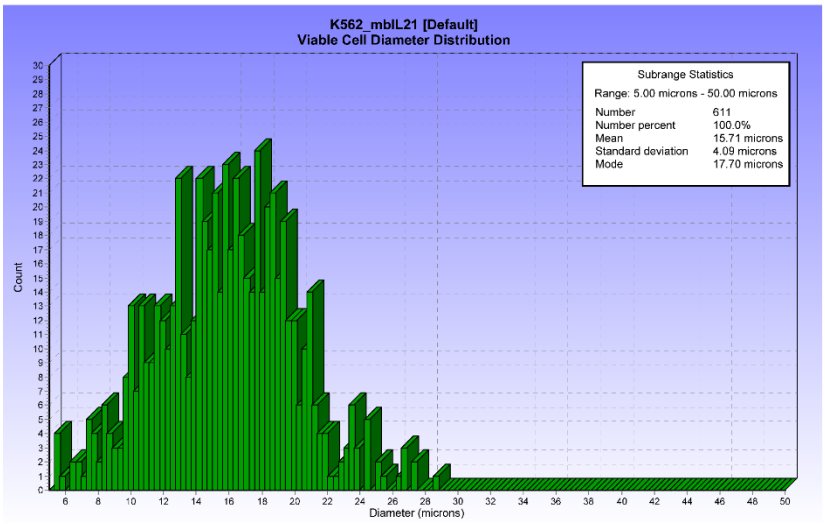

Figure 49: K562 Cell Diameter Distribution

Specific Consumption Rate of Glucose for Irradiated K562 Cells

K562 Cells were cultivated with RPMI-1640 media with 10% Fetal Bovine Serum. Cells were harvested and irradiated using a x-ray irradiator at a 10,000 cGy. Cells were cryopreserved in a cryotubes. At the point of thaw, K562 Cells were thawed, and cultivated in a T-75 flask with B0 media supplemented with 10% Human Serum. Cells number was measured on Day 0 and 2. Supernatant samples were taken on Day 0 and 2, and were measured the concentration of glucose.

Specific rate of glucose consumption at Day 1 was 7.13×10^{-10} mmol/cell/hour.

Cell concentration and glucose concentration were shown in Figure 50, Figure 51.

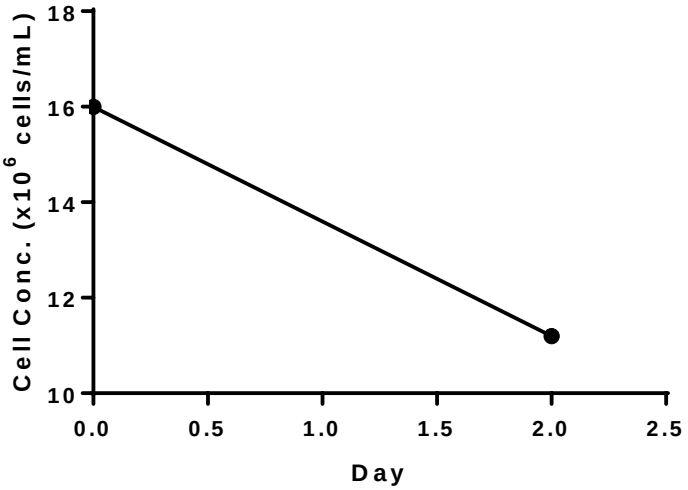

Figure 50: Cell Concentration of Irradiated K562

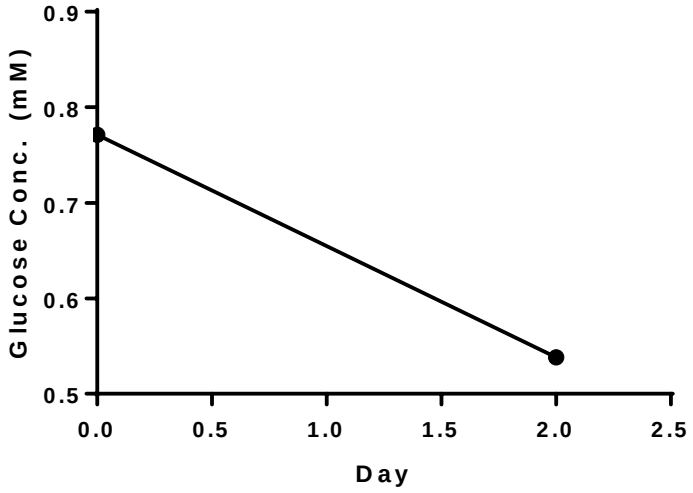

Figure 51: Glucose Concentration of Irradiated K562 Culture

4.7 INVESTIGATION OF MEDIA ON NK GROWTH BEHAVIOR

Nutrient Rich Chemically Defined Media

Blood from three donors were used. NK cells were isolated from PBMCs using magnetic beads for CD3 and CD19, making a heterogeneous population consists of NK cell and monocyte. The cells were placed in a T-75 flask at an initial concentration of 0.2 x 10^6 cells/mL. Irradiated K562.mbIL21 cells were thawed at an initial concentration of 0.4 x 10^6 cells/mL to stimulate NK cells. Media was replenished and NK cells were re-stimulated per the instruction in Materials and Methods.

The cells were cultivated using three different types of media. B0, CD013-22 (obtained from BioEngine, China), and a mixture of B0 and CD013-22 at a 1:1 ratio.

Figure 52 and Figure 53 show the amino acids composition of B0 and B0/CD013-22 (1:1 Mixture).

NK cell expansion profile is shown in Figure 54. NK cells expanded with B0 media showed the highest proliferation. The number of fold expansion at the end of two weeks cultivation using B0, CD013-22, B0/CD013-22 (1:1 Mixture) was 13603, 1041, 3616, respectively.

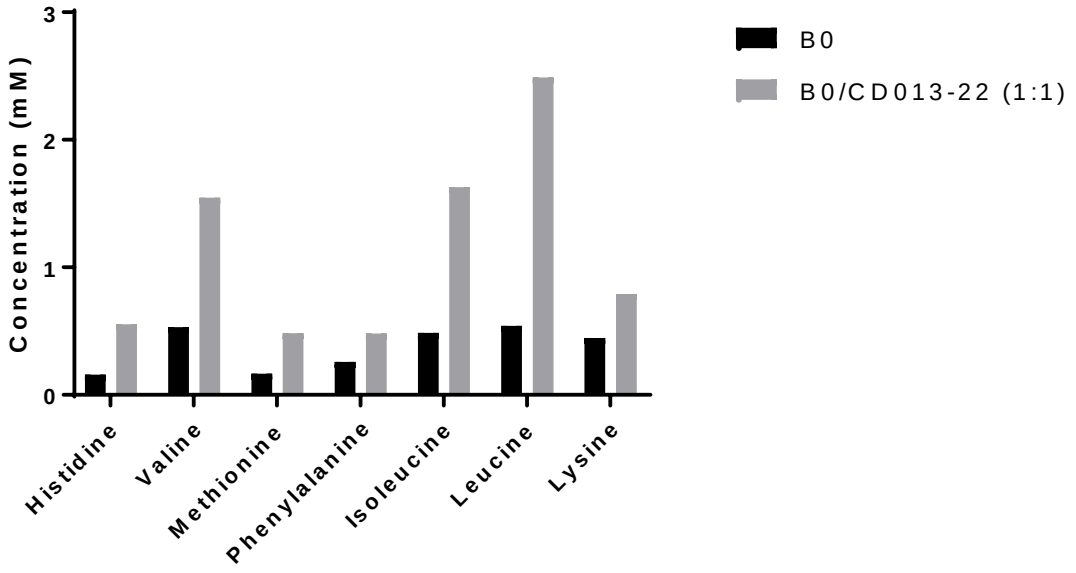

Figure 52: Essential Amino Acid Composition of B0 and B0/CD013-22 (1:1 Mixture)

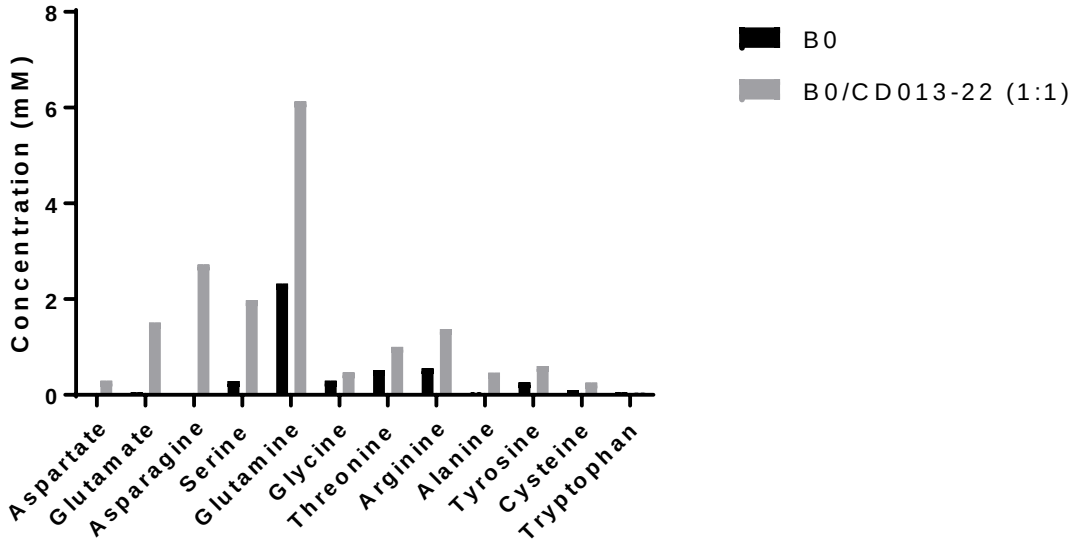

Figure 53: Non-Essential Amino Acid Composition of B0 and B0/CD013-22 (1:1 Mixture)

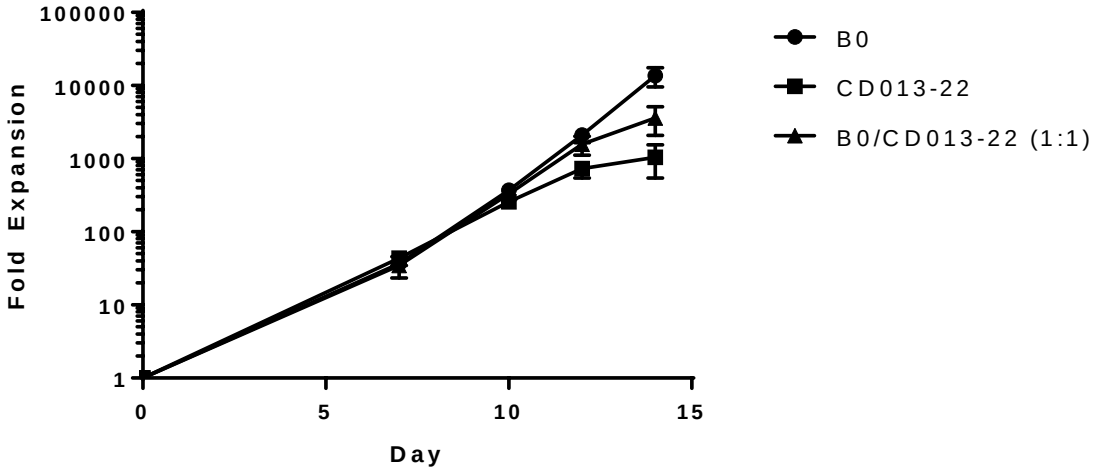

Figure 54: NK Cell Expansion Profile Using Media B0, CD013-22, B0/CD013-22 (1:1 Mixture)

Effect of K562 Supernatant on NK Cell Growth

In order to determine if there is effect on the molecules secreted from K562 during the cultivation, irradiated K562 cells were thawed in a T-75 flask at an initial concentration of 0.4 x 10^6 cells/mL. After three days of cultivation, cells were harvested, and the supernatant was filtered with a 0.2 µm Poly Ethylene Sulfone (PES) filter unit.

NK cells were isolated from one donor's PBMCs using magnetic bead for CD56 enrichment. Cells were placed in a 24 well plate at an initial cell concentration of 1 x 10^6 cells/mL. The supernatant was mixed with B0 media to generate three different kinds of conditioned medium: 0% Conditioned Media, 50% Conditioned Media, 100% Conditioned Media. 0% Conditioned Media contains 100% B0 media, and 100% Conditioned Media contains 0% B0 media.

The growth curve of NK cells cultured with different concentration of conditioned media was shown in Figure 55.

100% Conditioned Media, which is pure supernatant from K562 culture showed the highest proliferation compared to pure B0 media. However, the difference between three types of conditioned medium was not significant to determine the effect of the conditioned media.

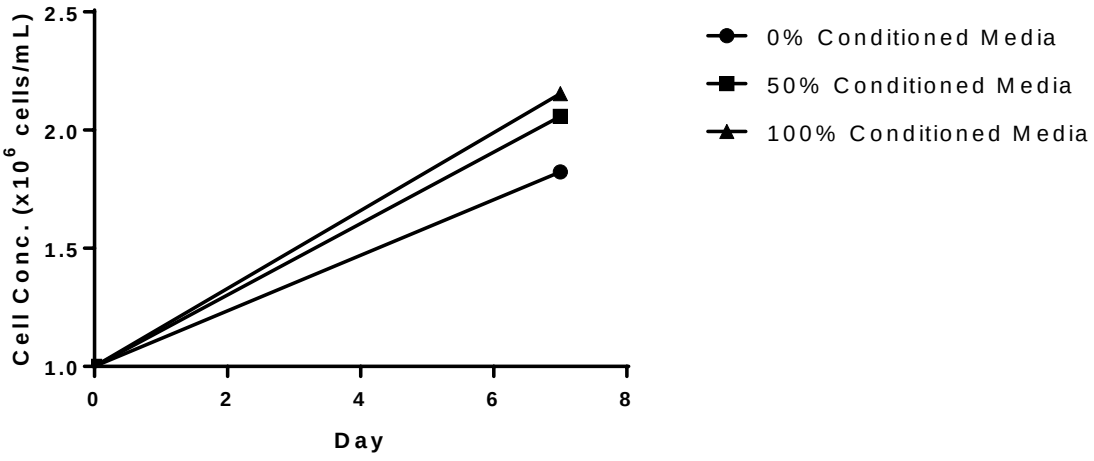

Figure 55: Growth Curve of NK Cells Cultivated with Varying Concentrations of Conditioned Media

4.8 COMPARISON OF GROWTH KINETICS IN VARYING SCALES

In conjunction with large scale experiments in T-75 flasks, small scale experiments were performed and analyzed by Jennifer One, advised by Prof. Samira Azarin, Department of Biomedical Engineering, University of Minnesota

NK cells were isolated from PBMCs of three donors using magnetic bead separation of CD56 cells. The cells were placed in 24 well plate and T-75 flask at an initial concentration of 0.31 x 10^6 cells/mL and 0.2 x 10^6 cells/mL, respectively. The cells were stimulated by irradiated K562.mbIL21 cells at a 1:1 ratio. For media change and re-stimulation by K562, T-75 followed the instructions in Materials and Methods. For 24 well plate, media was changed when the color of media changed from red to yellow, and the re-stimulation and dilution frequency were kept the same as the T-75 flask. The difference in the initial seeding density is coming from the difference in volume and the surface volume of the two different vessels, and

the number of cells per unit area was kept the same to mimic the identical culture conditions except the amount of media available per unit area.

Growth curves for both T-75 flask and 24 well plate are shown in Figure 56 and Figure 57.

In order to identify the effect of the difference in the amount of media and nutrient available per unit area, the number of fold expansion from the two difference vessels were compared in Figure 58. Overall expansion was comparable until Day 12. However, major difference in expansion occurred between Day 12 and 14, which requires further investigation.

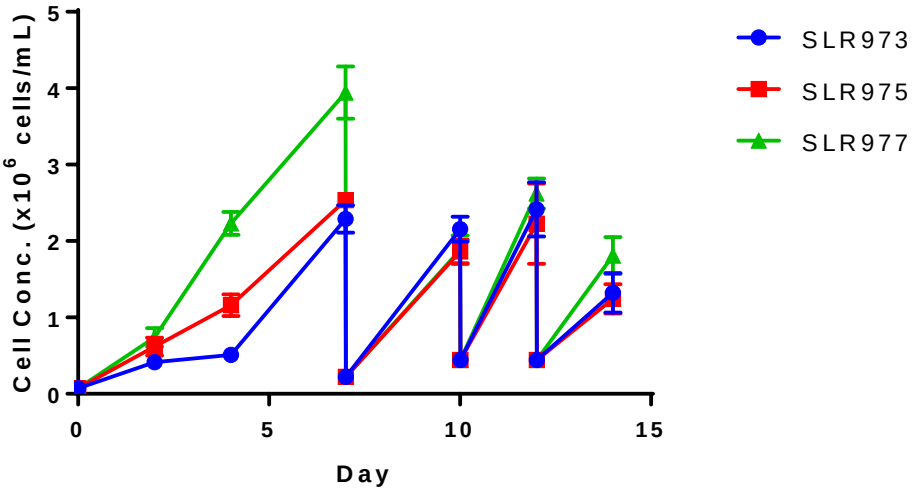

Figure 56: Growth Curve of NK Cells Cultured in 24 Well Plate with K562.mbIL21

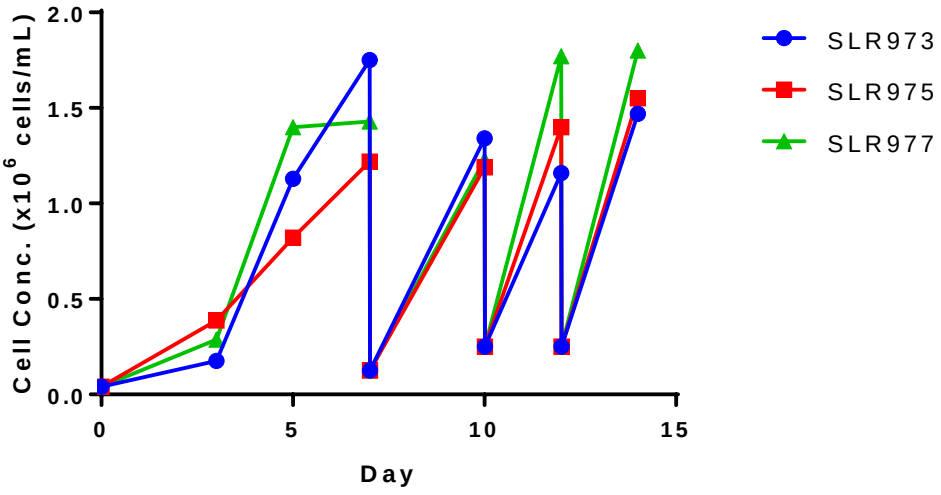

Figure 57: Growth Curve of NK Cells Cultured in T-75 Flask with K562.mbIL21

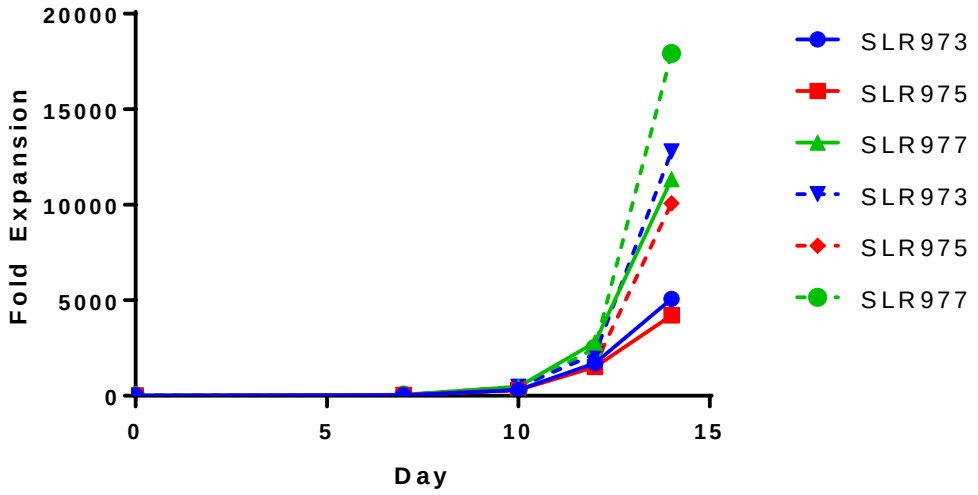

Figure 58: Cell Expansion Comparison Between NK Cells Cultivated in 24 Well Plate (Solid Line) and T-75 Flask (Dotted Line)

4.9 Effect of Stimulation by Live and Dead K562

In order to determine more details on the stimulation that NK cells receive from K562 cells, freshly isolated NK cells by depleting CD3 and CD19 cells were cultivated in T-75 flask using B0 media. One flask was stimulated by live K562.mbIL21 cells, and another flask was stimulated by dead K562.mbIL21 cells. The dead K562.mbIL21 cells were prepared by changing the medium that contained the cells to 35% Ethanol for 5 minutes. After 5 minutes period, the cells were washed with PBS, and transferred into the flask with NK cells. In terms of growth kinetics, NK cells cultivated with live and dead K562.mbIL21 cells showed similar growth. The growth curve is shown in Figure 59.

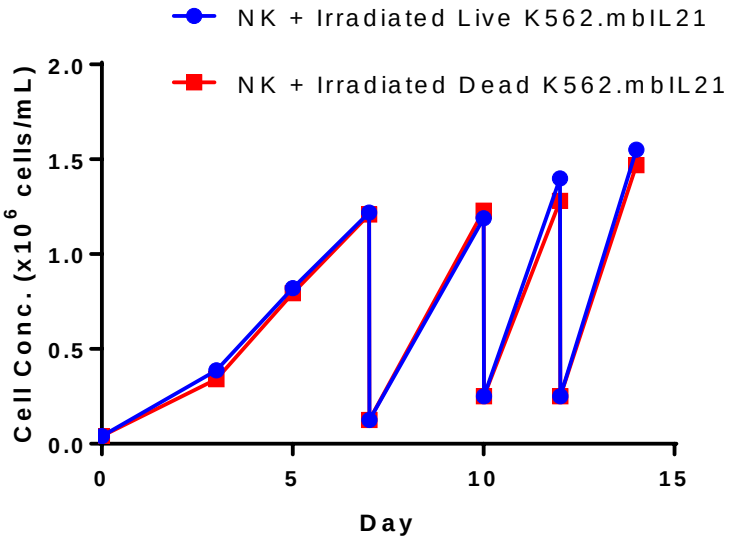

Figure 59: Growth Curve of NK Cells Cultivated with Live and Dead K562.mbIL21

Another experiment was conducted to determine the effect of stimulation by K562 further. NK cells were isolated from blood by depleting CD3 and CD19 cells, and were cultivated in T-75 flask. There were three different conditions tested, and their growth curve was shown in Figure 60. The condition shown in red line started with the co-cultivation of NK and K562.mbIL21, and the condition shown in blue line started without K562.mbIL21 stimulation. On Day 3, 10% volume of red and blue were exchanged so that red line contains 90% activated and 10% inactivated NK cells, whereas blue line contains 10% activated and 90% inactivated NK cells. Note here that small proportion of dead K562.mbIL21 cells and their debris were part of the volume that were transferred into the blue. This showed that those activated initially (blue) could expand when 10% volume of the red was transferred. It led us to suspect that dead K562 and their debris may attribute to expansion.

Green line in the figure shows a separate experiment that started initially with a co-cultivation of NK and K562.mbIL21 cells together. On Day 3, NK cells were isolated from the culture by using MACS Manual Separator (Miltenyi Biotec), which makes NK cells to be isolated from dead K562 and their debris. Isolated NK cells were transferred back to the flask to continue cultivation. Four additional days of cultivation showed slower growth compared to the blue line that contains 10% activated, 90% inactivated, plus dead K562 and their debris. The result shows to ascertain that physical contact to NK cells for the purpose of activation is critical factor for activation and expansion.

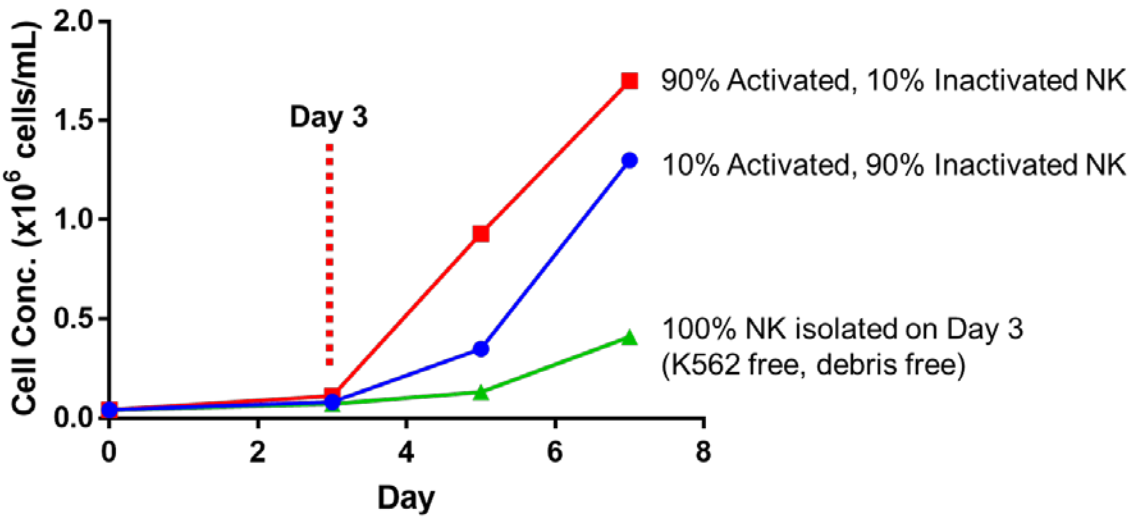

Figure 60: Growth Curve of NK cells Cultivated Varying Conditions of Stimulation

5 DISCUSSION

It is now evident that NK cells have capability to identify multiple targets using their activating and inhibitory receptor. Because of this characteristic, there will be a number of different tumors that can be treated with NK cells. Previous methods expanding the NK cells were limited due to lack of robust method that failed supplying sufficient number of cells for allogeneic therapies.

Recent advances in identifying and producing aAPCs helped greatly expanding the NK cells. While NK cells were being co-cultured with aAPCs, rapid expansion of NK cells and upregulation of their receptors were observed.

It is generally accepted that NK cells cultivated with cytokines are activated and are better to recognize and lyse the targets compared to inactivated NK cells. There are a number of publications discussing the effect of the cytokines in terms of their functionality (Caligiuri et al., 1990). This led the cytokines be a crucial part of NK cell expansion protocol.

Here we described and compared NK cell expansion using different kinds of membrane bound cytokines on K562. IL-2 and IL-15 are still used widely to expand and activate the NK cells, but the usage of IL-21 is somewhat limited due to lack of understanding of NK cell biology. The only known fact is that IL-15 is involved in signaling through STAT3 pathway, whereas IL-21 is involved in STAT5 pathway signaling. We showed that IL-21 membrane bound NK cells were able to expand as long as 35 days, and as much as 100 billion-fold expansion to provide cells for clinical purposes. This method provides advantages compared to the others in

terms of using media that does not require specialized culture media, and also does not require removal of T cell since the cultivation starts without any T cell population. These will lead to lower cost to manufacture NK cells since the cost of media and removal of T cell have been the costliest portion of NK cell production.

In addition to cell expansion, it is also important to highlight the upregulation of receptors during the co-cultivation as a result of activation of NK cells. We were able to identify upregulation of receptors, such as 3KIRs, NKp30, CD16, NKG2D, LFA-1, CD96, CD2, NKG2A, CD81, and CD45RO. Ideally, all receptors related to the functionality are activated when the cells are delivered to the patients, but it was also observed that each marker was upregulated at different time during the cultivation. Some were upregulated by Day 14, others were upregulated on Day 7 and slightly lost their expression on Day 14. This led to the need for a multi-dimensional analysis of the data.

SPADE analysis enabled us to overcome the limitation of conventional two-dimensional analysis. In this study, we defined and annotated the phenotype based on our observation from the two-dimensional analysis. However, there were many other cells that were clustered enough, but did not satisfy the intensity criterion previously defined. By using SPADE analysis, some phenotypes that were not able to be defined in two-dimension can be identified, and also some subtle population can be identified which will require further investigation. By taking a look at the detailed phenotypes of the nodes that were not part of any bubble, the criterion of phenotypes can be refined to give better analysis.

While it is important to focusing on NK cell expansion to provide a reliable method, the NK cells expanded with allogeneic feeder cells need to be purified to remove potential risks of infusing cancer cells into patient's body. Although the NK cells could be isolated from debris and allogeneic feeder cells, it could also be costly and make the overall process inefficient. Therefore, it will be our future objective to discover how NK cells can be expanded with safer allogeneic feeder cells or even without any feeder cells. It will require much deeper understanding NK cell biology and how NK cells get stimulated and expand *ex vivo* while they are in contact with the feeder cells.

There are more interests in cellular metabolism that it may be involved in NK cell responses and also expansion. Most of studies on lymphocyte metabolism are focusing on T cell. Detailed studies on NK cell metabolism is at a very emerging stage. By understanding how metabolism of NK cell changes during the activation and expansion may provide important hints to develop efficient methods to expand NK cells without feeder cells. We have measured glucose and oxygen consumption of NK cells that will pave a way to continue our efforts for metabolic flux analysis.

6 REFERENCES

Ahn, Y. O., Kim, S., Kim, T. M., Song, E. Y., Park, M. H., & Heo, D. S. (2013). Irradiated and activated autologous PBMCs induce expansion of highly cytotoxic human NK cells in vitro. *J Immunother, 36*(7), 373-381. doi:10.1097/CJI.0b013e3182a3430f

Apel, M., Bruning, M., Granzin, M., Essl, M., Stuth, J., Blaschke, J., . . . Huppert, V. (2013). Integrated Clinical Scale Manufacturing System for Cellular Products Derived by Magnetic Cell Separation, Centrifugation and Cell Culture. *Chemie Ingenieur Technik, 85*(1-2), 103-110. doi:10.1002/cite.201200175

Bamford, R. N., Grant, A. J., Burton, J. D., Peters, C., Kurys, G., Goldman, C. K., . . . Waldmann, T. A. (1994). The interleukin (IL) 2 receptor beta chain is shared by IL-2 and a cytokine, provisionally designated IL-T, that stimulates T-cell proliferation and the induction of lymphokine-activated killer cells. *Proc Natl Acad Sci U S A, 91*(11), 4940-4944.

Barkholt, L., Alici, E., Conrad, R., Sutlu, T., Gilljam, M., Stellan, B., . . . Dilber, M. S. (2009). Safety analysis of ex vivo-expanded NK and NK-like T cells administered to cancer patients: a phase I clinical study. *Immunotherapy, 1*(5), 753-764. doi:10.2217/imt.09.47

Caligiuri, M. A., Zmuidzinas, A., Manley, T. J., Levine, H., Smith, K. A., & Ritz, J. (1990). Functional Consequences of Interleukin-2 Receptor Expression on Resting Human-Lymphocytes - Identification of a Novel Natural-Killer-Cell Subset with High-Affinity Receptors. *Journal of Experimental Medicine, 171*(5), 1509-1526. doi:DOI 10.1084/jem.171.5.1509

Carlens, S., Gilljam, M., Chambers, B. J., Aschan, J., Guven, H., Ljunggren, H. G., . . . Dilber, M. S. (2001). A new method for in vitro expansion of cytotoxic human CD3(-)CD56(+) natural killer cells. *Human Immunology, 62*(10), 1092-1098. doi:Doi 10.1016/S0198-8859(01)00313-5

Carson, W. E., Giri, J. G., Lindemann, M. J., Linett, M. L., Ahdieh, M., Paxton, R., . . . Caligiuri, M. A. (1994). Interleukin (IL) 15 is a novel cytokine that activates human natural killer cells via components of the IL-2 receptor. *J Exp Med, 180*(4), 1395-1403.

Couzin, J. (2002). Cancer immunotherapy. Select T cells, given space, shrink tumors. *Science, 297*(5589), 1973. doi:10.1126/science.297.5589.1973a

Denman, C. J., Senyukov, V. V., Somanchi, S. S., Phatarpekar, P. V., Kopp, L. M., Johnson, J. L., . . . Lee, D. A. (2012). Membrane-bound IL-21 promotes sustained ex vivo proliferation of human natural killer cells. *PLoS One, 7*(1), e30264. doi:10.1371/journal.pone.0030264

Felices, M., Lenvik, A., Chu, S., McElmurry, R., Cooley, S., Tolar, J., . . . Miller, J. S. (2016). Continuous IL-15 Signaling Leads to Functional Exhaustion of Human Natural Killer Cells through Metabolic Changes That Alters Their In Vivo Anti-Tumor Activity. *Blood, 128*(22).

Fujisaki, H., Kakuda, H., Shimasaki, N., Imai, C., Ma, J., Lockey, T., . . . Campana, D. (2009). Expansion of highly cytotoxic human natural killer cells for cancer

cell therapy. *Cancer Res, 69*(9), 4010-4017. doi:10.1158/0008-5472.CAN-08-3712

Geller, M. A., Cooley, S., Judson, P. L., Ghebre, R., Carson, L. F., Argenta, P. A., . . . Miller, J. S. (2011). A phase II study of allogeneic natural killer cell therapy to treat patients with recurrent ovarian and breast cancer. *Cytotherapy, 13*(1), 98-107. doi:10.3109/14653249.2010.515582

Grabstein, K. H., Eisenman, J., Shanebeck, K., Rauch, C., Srinivasan, S., Fung, V., . . . et al. (1994). Cloning of a T cell growth factor that interacts with the beta chain of the interleukin-2 receptor. *Science, 264*(5161), 965-968.

Granzin, M., Wagner, J., Kohl, U., Cerwenka, A., Huppert, V., & Ullrich, E. (2017). Shaping of Natural Killer Cell Antitumor Activity by Ex Vivo Cultivation. *Front Immunol, 8*, 458. doi:10.3389/fimmu.2017.00458

Huenecke, S., Zimmermann, S. Y., Kloess, S., Esser, R., Brinkmann, A., Tramsen, L., . . . Koehl, U. (2010). IL-2-driven regulation of NK cell receptors with regard to the distribution of CD16+ and CD16- subpopulations and in vivo influence after haploidentical NK cell infusion. *J Immunother, 33*(2), 200-210. doi:10.1097/CJI.0b013e3181bb46f7

Kim, E. K., Ahn, Y. O., Kim, S., Kim, T. M., Keam, B., & Heo, D. S. (2013). Ex vivo activation and expansion of natural killer cells from patients with advanced cancer with feeder cells from healthy volunteers. *Cytotherapy, 15*(2), 231-241 e231. doi:10.1016/j.jcyt.2012.10.019

Koepsell, S. A., Miller, J. S., & McKenna, D. H., Jr. (2013). Natural killer cells: a review of manufacturing and clinical utility. *Transfusion, 53*(2), 404-410. doi:10.1111/j.1537-2995.2012.03724.x

Kotecha, N., Krutzik, P. O., & Irish, J. M. (2010). Web-based analysis and publication of flow cytometry experiments. *Curr Protoc Cytom, Chapter 10*, Unit10 17. doi:10.1002/0471142956.cy1017s53

Lapteva, N., Durett, A. G., Sun, J., Rollins, L. A., Huye, L. L., Fang, J., . . . Rooney, C. M. (2012). Large-scale ex vivo expansion and characterization of natural killer cells for clinical applications. *Cytotherapy, 14*(9), 1131-1143. doi:10.3109/14653249.2012.700767

Levine, B. L., Miskin, J., Wonnacott, K., & Keir, C. (2017). Global Manufacturing of CAR T Cell Therapy. *Mol Ther Methods Clin Dev, 4*, 92-101. doi:10.1016/j.omtm.2016.12.006

Ljunggren, H. G., & Karre, K. (1990). In search of the 'missing self': MHC molecules and NK cell recognition. *Immunol Today, 11*(7), 237-244.

McMichael, E. L., Jaime-Ramirez, A. C., Guenterberg, K. D., Luedke, E., Atwal, L. S., Campbell, A. R., . . . Carson, W. E. (2017). IL-21 Enhances Natural Killer Cell Response to Cetuximab-Coated Pancreatic Tumor Cells. *Clinical Cancer Research, 23*(2), 489-502. doi:10.1158/1078-0432.Ccr-16-0004

Meyer-Monard, S., Passweg, J., Siegler, U., Kalberer, C., Koehl, U., Rovo, A., . . . Tichelli, A. (2009). Clinical-grade purification of natural killer cells in haploidentical hematopoietic stem cell transplantation. *Transfusion, 49*(2), 362-371. doi:10.1111/j.1537-2995.2008.01969.x

Miller, J. F., & Sadelain, M. (2015). The journey from discoveries in fundamental immunology to cancer immunotherapy. *Cancer Cell, 27*(4), 439-449. doi:10.1016/j.ccell.2015.03.007

Miller, J. S., Oelkers, S., Verfaillie, C., & McGlave, P. (1992). Role of monocytes in the expansion of human activated natural killer cells. *Blood, 80*(9), 2221-2229.

Parkhurst, M. R., Riley, J. P., Dudley, M. E., & Rosenberg, S. A. (2011). Adoptive transfer of autologous natural killer cells leads to high levels of circulating natural killer cells but does not mediate tumor regression. *Clin Cancer Res, 17*(19), 6287-6297. doi:10.1158/1078-0432.CCR-11-1347

Pierson, B. A., Miller, J. S., Verfaillie, C., McGlave, P. B., & Hu, W. S. (1994). Population dynamics of human activated natural killer cells in culture. *Biotechnol Bioeng, 43*(8), 685-692. doi:10.1002/bit.260430803

Siegler, U., Meyer-Monard, S., Jorger, S., Stern, M., Tichelli, A., Gratwohl, A., . . . Kalberer, C. P. (2010). Good manufacturing practice-compliant cell sorting and large-scale expansion of single KIR-positive alloreactive human natural killer cells for multiple infusions to leukemia patients. *Cytotherapy, 12*(6), 750-763. doi:10.3109/14653241003786155

Smyth, M. J., Cretney, E., Kelly, J. M., Westwood, J. A., Street, S. E., Yagita, H., . . . Hayakawa, Y. (2005). Activation of NK cell cytotoxicity. *Mol Immunol, 42*(4), 501-510. doi:10.1016/j.molimm.2004.07.034

Sutlu, T., Stellan, B., Gilljam, M., Quezada, H. C., Nahi, H., Gahrton, G., & Alici, E. (2010). Clinical-grade, large-scale, feeder-free expansion of highly active human natural killer cells for adoptive immunotherapy using an automated bioreactor. *Cytotherapy, 12*(8), 1044-1055. doi:10.3109/14653249.2010.504770

Vera, J. F., Brenner, L. J., Gerdemann, U., Ngo, M. C., Sili, U., Liu, H., . . . Rooney, C. M. (2010). Accelerated production of antigen-specific T cells for preclinical and clinical applications using gas-permeable rapid expansion cultureware (G-Rex). *J Immunother, 33*(3), 305-315. doi:10.1097/CJI.0b013e3181c0c3cb

Vivier, E., Tomasello, E., Baratin, M., Walzer, T., & Ugolini, S. (2008). Functions of natural killer cells. *Nat Immunol, 9*(5), 503-510. doi:10.1038/ni1582

Walzer, T., Jaeger, S., Chaix, J., & Vivier, E. (2007). Natural killer cells: from CD3(-)NKp46(+) to post-genomics meta-analyses. *Curr Opin Immunol, 19*(3), 365-372. doi:10.1016/j.coi.2007.04.004

Yang, Y., Jacoby, E., & Fry, T. J. (2015). Challenges and opportunities of allogeneic donor-derived CAR T cells. *Curr Opin Hematol, 22*(6), 509-515. doi:10.1097/MOH.0000000000000181